ANALYSIS AND OPTIMUM DESIGN OF AXISYMMETRIC PLATES AND SHELLS

A MASTER'S THESIS

in

Civil Engineering

University of Gaziantep

By

Murat TURAL

January 2005

Approval of the Graduate School of Natural and Applied Sciences

Prof. Dr. Sadettin ÖZYAZICI
Director

I certify that this thesis satisfies all the requirements as a thesis for the degree of Master of Science.

Assist. Prof. Dr. Hanifi ÇANAKÇI
Chairman of the Department

I certify that I have read this thesis and that in my opinion it is fully adequate, in scope and quality, as a thesis for the degree of Master of Science.

Prof. Dr. Mustafa ÖZAKÇA
Supervisor

Examining Committee in Charge:

Prof. Dr. Mustafa ÖZAKÇA ....

Assoc. Prof. Dr. İbrahim H. GÜZELBEY (Chairman) ....

Assist. Prof. Dr. Mustafa GÜNAL ....

ABSTRACT

ANALYSIS AND OPTIMUM DESIGN OF
AXISYMMETRIC PLATES AND SHELLS

TURAL, Murat
M.S. in Civil Engineering
Supervisor: Prof. Dr. Mustafa ÖZAKÇA
January 2005, 68 pages

This thesis deals with the development of reliable and efficient computational tools to analyze and find optimum shapes of axisymmetric plates and shells in static, free vibration and buckling situations. The finite element method is used to determine the stresses, displacements, natural frequencies and critical buckling loads based on Mindlin-Reissner shell theory. An automated analysis and optimization procedure is adopted which integrates finite element analysis, parametric cubic spline geometry definition, automatic mesh generation, sensitivity analysis and mathematical programming methods.

Key words: Axisymmetric plates and shells, static analysis, free vibration analysis, buckling analysis, shape optimization.

ÖZET

AKSİMETRİK PLAK VE KABUK YAPILARIN ANALİZİ VE OPTİMUM TASARIMI

TURAL, Murat
Yüksek Lisans Tezi, İnşaat Müh. Bölümü
Tez Yöneticisi: Prof. Dr. Mustafa ÖZAKÇA
Ocak 2005, 68 sayfa

Bu tez, aksimetrik plak ve kabuk yapıların statik, serbest titreşim ve burkulma analizleri ve optimizasyonu için güvenilir ve verimli bir bilgisayar programı geliştirilmesini kapsamaktadır. Mindlin-Reissner kabuk teorisine bağlı sonlu elemanlar metodu kullanılarak gerilmeler, şekil değiştirmeler, doğal frekans titreşim şekilleri ve burkulma yükleri hesaplanmıştır. Sonlu elemanlar metodu, kübik eğrilerle geometri tanımlama, ağ üretimi, hassasiyet analizi ve matematik programlama metotlarını birleştiren otomatik analiz ve optimizasyon tekniği uygulanmaktadır.

Anahtar kelimeler: Aksimetrik plak ve kabuklar, statik analiz, serbest titreşim analizi, burkulma analizi, şekil optimizasyonu

ACKNOWLEDGEMENTS

I would like to express my sincere and gratitude thanks to my supervisor, Prof. Dr. Mustafa Özakça, for his guidance, advice, encouragement and suggestions during the preparation of this thesis.

My special thanks are reserved for my father, my project manager, Dara Palaoğlu and Dr. Nildem Tayşi for their encouragement, understanding, patience and great help.

TABLE OF CONTENTS

LIST OF TABLES

LIST OF FIGURES

LIST OF SYMBOLS

Abbreviations:

CAD	Computer Aided Design
DOF	Degrees Of Freedom
FD	Finite Difference
FE	Finite Element
MMA	Method of Moving Asymptotes
MR	Mindlin-Reissner
SE	Strain Energy

Latin Symbols:

Scalar

A	area
b	length of strip
C_p, S_p	cosine and sine function
$C(0)$	order of continuity
d	displacement
E	Young's modulus
$f_{ui}^{p}, f_{vi}^{p}, f_{wi}^{p}$	forces associated with u, v and w and harmonic p
$f_{\phi i}^{p}, f_{\psi i}^{p}$	forces associated with ϕ and ψ and harmonic p
$F(\mathbf{s})$	objective function to be minimized
$\overline{F}_u, \overline{F}_v, \overline{F}_w$	distributed line forces
$\overline{F}_\phi, \overline{F}_\psi$	distributed line couples
G	modulus of rigidity

$g_j(\mathbf{s})$	inequality constraint function
g_u, g_v, g_w	distributed loadings associated with u, v and w displacement
g_ϕ, g_ψ	distributed loadings associated with ϕ and ψ displacement
$h_k(\mathbf{s})$	equality constraint function
I	total virtual work
I^e	total work from strip (or element) e
J	Jacobian
k	elastic foundation modulus
ℓ	the arc length parameter of the curve
L	span length
(m,n)	mode and half-sine wave
M_l, M_y, M_{ly}	stress resultant due to bending
N_i	shape function associated with node i
N_l, N_y, N_{ly}	membrane stress resultant
n_{dv}	number of design variables
Q_l, Q_y	shear forces
r,z	radial and vertical coordinate
R	radius of curvature
$\mathbf{s}$	design variables
t	thickness
t_i	thickness at node i
u_ℓ, v_ℓ, w_ℓ	displacement components in ℓ, y and n-direction
u, v, w	global displacement parameters
u^p, v^p, w^p	displacement amplitudes of p^{th} harmonic
$\lVert\mathbf{W}\rVert^2$	total strain energy
$\lVert\mathbf{W}\rVert_b^{p\,2}$	strain energy for p harmonic due to bending
$\lVert\mathbf{W}\rVert_m^{p\,2}$	strain energy for p harmonic due to membrane
$\lVert\mathbf{W}\rVert_s^{p\,2}$	strain energy for p harmonic due to shear
x_i, y_i, z_i	typical cartesian coordinates of node i
x, y, z	global cartesian coordinates

Vector

$\mathbf{d}$	vector of unknown displacements (eigenvector)
$\mathbf{d}_i^p$	vector of nodal degrees of freedom
$\mathbf{d}_i^e$	displacement (eigenvector) vector associated with element *e* and node *i*
$\overline{\mathbf{d}}_i^p$	displacement (eigenvector) vector at node *i* and harmonic *p*
$\mathbf{f}$	vector of structural load
$\{\mathbf{f}_i^e\}^p$	nodal force vector associated with node *i* and harmonic *p*
$\mathbf{g}$	vector of distributed loading
$\mathbf{u}$	displacement field vector

Matrix

$\mathbf{B}$	strain-displacement matrix
$\mathbf{B}_{mi}^e$	membrane strain-displacement matrix for element *e* and node *i*
$\mathbf{B}_{bi}^e$	bending strain-displacement matrix for element *e* and node *i*
$\mathbf{B}_{si}^e$	shear strain-displacement matrix for element *e* and node *i*
$\mathbf{B}_{mi}^p$	membrane strain-displacement matrix for node *i* and harmonic *p*
$\mathbf{B}_{bi}^p$	bending strain-displacement matrix for node *i* and harmonic *p*
$\mathbf{B}_{si}^p$	shear strain-displacement matrix for node *i* and harmonic *p*
$\overline{\mathbf{B}}_{mi}, \overline{\mathbf{B}}_{bi}, \overline{\mathbf{B}}_{si}$	transformed strain-displacement matrices
$\mathbf{B}_{pi}$	in-plane strain displacement matrix
$\mathbf{B}_{si}$	shear strain displacement matrix
$\mathbf{D}$	matrix of rigidities
$\mathbf{D}_m$, $\mathbf{D}_b$, $\mathbf{D}_s$	matrices of membrane, bending and shear rigidities

$\mathbf{D}_p$, $\mathbf{D}_s$	in-plane and transverse elasticity matrix
$\mathbf{J}$	Jacobian matrix
$\mathbf{K}^e_{ij}$	stiffness matrix associated with element e and node i and j
$[\mathbf{K}]^{pp}$	global stiffness matrix associated with harmonic p
$[\mathbf{K}^e_{ij}]^{pq}$	stiffness matrix linking nodes i and j and harmonics p and q
$[\overline{\mathbf{K}}^e_{ij}]^{pq}$	elastic foundation stiffness matrix for nodes i and j and p and q
$\mathbf{K}$	symmetric, banded stiffness matrix
$\mathbf{K}^e_{mij}$	membrane stiffness matrix for element e and node i and j
$\mathbf{K}^e_{bij}$	bending stiffness matrix for element e and node i and j
$\mathbf{K}^e_{sij}$	shear stiffness matrix for element e and node i and j
$\mathbf{M}$	global mass matrix
$\mathbf{M}^e_{ij}$	mass matrix associated with element e and node i and j
$[\mathbf{M}]^{pp}$	global mass matrix associated with harmonic p
$[\mathbf{M}^e_{ij}]^{pq}$	mass matrix linking nodes i and j and harmonics p and q
$\mathbf{N}$	shape function matrix
$\mathbf{T}$	transformation matrix

Greek Symbols:

α	angle between local and global axes
β	arch opening angle
δ_t	mesh density
Δs_k	small perturbation of design variables s_k
$\boldsymbol{\varepsilon}_m, \boldsymbol{\varepsilon}_b, \boldsymbol{\varepsilon}_s$	membrane, bending and transverse shear strain vectors
$\varepsilon_\ell, \varepsilon_y$	strain in ℓ direction and longitudinal strain
$\gamma_{\ell y}, \gamma_{yn}$	shear strain
κ	shear modification factor
κ_ℓ	curvature in the ℓ-direction

κ_y	longitudinal curvature
$\kappa_{\ell y}$	twisting curvature
ν	Poisson's ratio
ω	fundamental frequency
ϕ, ψ	rotation of the midsurface normal in the ℓn and yn plane
ϕ^p, ψ^p	rotation amplitude for the p^{th} harmonic term
ξ, η, ζ	isoparametric element natural (curvilinear) coordinates
σ	stress component
$\boldsymbol{\sigma}_m^p, \boldsymbol{\sigma}_b^p, \boldsymbol{\sigma}_s^p$	membrane, bending and shear stress resultant vectors
ρ	mass density
$\partial\ell$	partial differential of ℓ

CHAPTER 1

INTRODUCTION

1.1 General Information

Plate and shell structures constitutes an important class of problems in civil, mechanical and aeronautical engineering in order to avoid unexpected catastrophic failures and to produce efficient and reliable designs, computational tools have been developed for analysis and shape optimization processes.

For precise solutions in analysis process, the finite element method (FE) is well established and is regarded as a most powerful and versatile tool. The basic philosophy is to discretize the structures and interpolate the behavior by finite element method. Many research activities took place in this area investigating the applicability and developing many useful extensions. However, there are still the necessity and capability of further improvements, as shown in this present work.

In structural design, it is necessary to obtain an approximate layout of a structure so that it can carry the imposed loads safely and economically. Optimization is a valuable tool to generate efficient innovative layouts for structures which go beyond the experience of the designer. The objective of optimization is often to produce minimum volume structures with maximum stability, strength and stiffness by changing the layout within a specified design domain and subject to a set of support and load conditions.

Optimization process starts with a design specification where, among other data, the performance of a part to be designed is laid down. Then starting from an idea or basic concept a design is carried out using modeling tool and computational analysis technique such as the FE method are used for the calculation of the structural response. Sensitivities to changes in design are evaluated using numerical techniques and established optimization techniques are employed to produce optimal designs using iterative procedures.

1.2 Principal Objectives

The main motivations of the thesis are static, free vibration, buckling analysis and Structural Shape Optimization (SSO) of axisymmetric plates and shells using reliable and efficient computational tools. The specific objectives of this thesis may be expressed as follows:

- to study a new static, free vibration, and buckling analysis and shape optimization procedure
- to analyze axisymmetric plate and shell structures with different boundary conditions;
- to illustrate the accuracy and relative performance of a family of linear, quadratic and cubic finite elements by comparing with other numerical solutions;
- to obtain the best geometric shape and thickness variation for axisymmetric plates and shells so that it can meet the predefined constraints.

1.3 About Computer Program

In this thesis, the intention is to deal with shells idealizations problem involving buckling. A free vibration analysis and shape optimization programs for straight planform folded plates and shells were developed by Özakça [1]. These programs are used to carry out static, free vibration and buckling analysis of axisymmetric shell structures. The program is presented to assist structural engineer to design structurally, efficient forms and provide considerable insight into the structural behavior. The following changes are done in the program:

- Analysis and optimization are integrated in one program.
- A mathematical programming method, MMA and DOT is integrated to the program.
- The capability of the present program is increased such as program can handle different objective function and constraints.
- Program is written in FORTRAN 90 using double precision and run on personal computers.

1.4 Layout of Thesis

The contents of each chapter are now described:

- In Chapter 2, literature survey about static, free vibration and buckling analysis and optimizations are given.
- The basic finite element formulation for static, free vibration and buckling analysis of shells of revolution is presented and verified in Chapter 3.
- In Chapter 4, several examples of static, free vibration and buckling analysis of shells of revolution are presented and results obtained are compared with previous published results.
- Chapter 5, deals with the optimization process which include the definition, the design variables, the sensitivity analysis and the optimization algorithm.
- In Chapter 6, several examples of axisymmetric plates and shells are presented to illustrate structural shape optimization.
- Finally in Chapter 7, conclusions based on the present work are outlined and suggestions for future work are discussed.

CHAPTER 2

LITERATURE SURVEY

2.1 Analysis

Shell structures have many applications including cooling towers, liquid-retaining structures and roofs where large uninterrupted space is required. These structures are aesthetically pleasing, make efficient use of construction materials and can economically meet design criteria. A number of serious failures of shell structures during the last century have led to significant research into their behavior, analysis, design and construction. Despite this, further research is still required to improve design, especially with respect to shell dynamics and stability.

Much research into the behavior of hyperbolic axisymmetric shell structures has been carried out since the development of the finite-element method. Areas of interest during the last few decades have included static and pseudo-static effects of wind and earthquake loading, thermal effects, structural stability, non-linear analysis, durability, limit-state loading, construction material and techniques, foundation settlement and idealization of the supporting members at the base. This previous research has concentrated on shell behavior under static loading and hence providing limited knowledge on the dynamic behavior and stability.

Axisymmetric shell structures, generated by rotating a plane curve generator around an axis of rotation to form a circumferentially closed surface, have many applications such as hyperbolic cooling towers, cylindrical or conical liquid-retaining structures and spherical dome roofs. These structures are thin, and due to their curvature, are not only aesthetically pleasing but also have adequate strength [2–4]. It will be found that considerable simplification can be achieved if account is taken of axial symmetry of the structure. In particular, if both the shell and the loading are axisymmetric it will be found that the elements become *one dimensional*. Analysis of thin wall axisymmetric structures based on the thick and thin plate and shell theories can be classified into two main groups: analytical methods and numerical methods.

2.1.1 Analytical methods

The limitations imposed by analytical techniques are well known. Only in special cases of loading, plate geometry and edge conditions is closed form solution possible [5,6]. Classical analytical techniques are not suitable for plates and shells with an abrupt change of thickness, complex geometry and mixed boundary conditions. Approximate methods are therefore not only permissible but, in many cases, are the only means of solution to this problem.

2.1.2 Numerical methods

Due to severe economic constraints and stringent deadlines coupled with the enormous growth in computer speed and power, engineers are resorting to numerical methods for analysis of plates and shells. Among the various numerical methods, finite element method becomes firmly established as engineering tools for linear analysis of shells.

The first approach to the finite element solutions of axisymmetric shells was presented by Grafton and Strome [7]. In this, the elements are simple conical frustra and a direct approach via displacement functions is used. Later much work was accomplished to extend the processes to curved elements and indeed to refine the approximations involved. The literature on the subject is considerable amount. We now provide a brief and selective review of the literature on analysis of axisymmetric structures which is limited to the type of analysis considered in this thesis.

2.1.2.1 Static analysis

Isoparametric MR elements for shells of revolution have been developed by Zienkiewicz et al. [8] in which transverse shear deformation is taken into account. Recently, Day and Potts [9] highlighted the drawbacks of the formulation on which the two-node element, developed by Zienkiewicz et al. [8], is based and presented a new approach which provides an accurate solution for the analysis of general shells of revolution.

A boundary element is presented for purely axisymmetric elasticity with arbitrary body force by Park [10]. The particular integrals for displacement and traction were derived by integrating three-dimensional ones along the circumferential direction.

A local–global finite element technique, suitable for the analysis of shells of revolution with localized non-axisymmetric effects such as cracks, cutouts and column supports, was presented by Gould and Hara [11]. Both material and geometrical nonlinearities were considered. The model combined, in a single analysis, rotational shell elements, general shell elements, and column elements. Rotational shell elements were employed in the axisymmetric portion of the shell, where the nonaxisymmetric behavior in loading and deformation was accounted for by including appropriate Fourier harmonics. In the local zone, where deviations from axisymmetry were contained, a general isoparametric shell element was employed. Continuity of displacements between the rotational and general shell elements was achieved either by a layer of transitional elements or by a direct coordinate transformation. If the shell was supported on a discrete system of columns, a standard 3 dimensional beam element with six Degrees of Freedom (DOF) per node was deployed.

Liu et al. [12] presented exact axisymmetric bending solutions for linearly tapered, annular Mindlin plates with various boundary conditions for the inner and outer edges. The Mindlin plate theory has been adopted so as to incorporate the elect of transverse shear deformation which becomes significant in tapered and thick plates.

A numerical method for the structural analysis of laminated axisymmetric shells based on the high-order theory was presented Correia et al. [13]. A higher order displacement field was used with the longitudinal and circumferential components of the displacement given by power series of the transversal coordinate and the condition of zero stress in the top and bottom surfaces of the shell was imposed. In the element formulation the circumferential dependence was carried out by expanding the dependent variables and loading in truncated Fourier series which leads to a semi-analytical element.

2.1.2.2 Free vibration analysis

Without assuming displacement models and stress distribution, the mixed state equation for the axisymmetric problem of the thick laminated closed cantilever cylindrical shells was established by means of weak formulation of equilibrium equations including boundary conditions in a cylindrical coordinate system by Ding and Tang [14]. The exact solution was obtained for thick laminated closed cantilever cylindrical shells. All equations of elasticity were satisfied and all elastic constants were taken into account.

Benjeddou [15] presented and evaluates a local-global B-spline finite element method for the modal analysis of joined thin shells of revolution. Each shell component was modeled by a super element. For smooth meridian, local displacements of the shell middle surface and their first derivatives were matched at the junction. However, for discontinuous shells, the $C(1)$ continuity of tangential displacements was relaxed and a local to global frame transformation was applied for normal and longitudinal displacements. Efficiency and accuracy of the proposed technique were evaluated through various well known two-branch shell combinations.

An efficient substructuring analysis method was presented for predicting the natural frequencies of shells of revolution which may have arbitrary shape of meridian, general type of material property and any kind of boundary condition. This method was developed in the context of first order shear deformation shell theory as well as the classical thin shell theory. The vibrational behaviors of a circular cylinder, an elliptic hyperboloid shell "modeling a cooling tower" and a complete spherical shell were investigated using this method.

Free axisymmetric vibration of simply supported isotropic circular plates was investigated by using the energy method and a multimode approach by Haterbouch and Benamar [16]. In-plane deformation was included in the formulation. Lagrange's equations were used to derive the governing equation of motion. Using the harmonic balance method, the equation of motion were converted into a algebraic form. The numerical iterative method of solution adopted was the so-called linearized updated mode method, which permits the authors to obtain accurate results for vibration amplitudes up to three times the plate thickness. The percentage of participation of each out-of-plane basic function to the deflection shape and to the bending stress at the plate centre and of each in-plane basic function to the membrane stress at the centre were calculated in order to determine the minimum number of in- and out-of-plane basic functions to be used in order to achieve a good accuracy of the model.

An exact closed-form solution was derived for an axisymmetrically vibrating inhomogeneous circular plate that was simply supported at its boundary by Elishakoff and Storch [17]. The solution was characterized as an unusual one since for its counterpart—the homogeneous plate, transcendental functions were called for whereas a solution was found in elementary functions, namely, polynomials. The analysis was based on an inverse vibration problem: Given a candidate mode shape and density distribution, they calculated the plate stiffness so that the governing equation for the plate mode shape was identically satisfied.

A three-dimensional free vibration analysis of circular and annular plates was presented via the Chebyshev–Ritz method by Zhou et al. [18]. The solution procedure was based on the linear, small strain, three-dimensional elasticity theory. Selecting Chebyshev polynomials which could be expressed in terms of cosine functions as the admissible functions, a convenient governing eigenvalue equation could be derived through the Ritz method. According to the geometric properties of circular and annular plates, the vibration was divided into three distinct categories: axisymmetric vibration, torsional vibration and circumferential vibration. Each vibration category could be further subdivided into the antisymmetric and symmetric ones in the thickness direction.

Nasir et al. [19] treated the free vibration and seismic response of hyperbolic shells, and examines the influence of thickness, height and curvature on this response. Analysis has been undertaken using the finite element method.

Axisymmetric shells were analyzed by means of one-dimensional continuum elements by using the analogy between the bending of shells and the bending of beams on elastic foundation by Cela et al. [20]. The mathematical model was formulated in the frequency domain. The solution of the governing equations of vibration of beams were exact, the spatial discretization only depends on geometrical or material considerations.

2.1.2.3 Buckling analysis

Ley et al. [21] developed the analysis to predict buckling loads of ring-stiffened anisotropic cylinders subject to axial compression, torsion and internal pressure. Buckling displacements are represented by a Fourier series in the circumferential coordinate and the finite-element method in the axial coordinate.

The third-order shear deformation plate theory was employed to solve the axisymmetric bending and buckling problems of functionally graded circular plates by Ma and Wang [22]. Relationships between the third-order shear deformation plate theory solutions of axisymmetric bending and buckling of functionally graded circular plates and those of isotropic circular plates based on the classical plate theory were presented, from which one could easily obtain the third-order shear deformation plate theory solutions for the axisymmetric bending and buckling of functionally graded plates. It was assumed in analysis that the mechanical properties of the functionally graded plates vary continuously through the thickness of the plate and obey a power law distribution of the volume fraction of the constituents. Effects of material gradient property and shear deformation on the bending and buckling of

functionally graded plates were discussed in the frameworks of the first-order plate theory and third-order plate theories.
Wang et al. [23] extended their earlier work and studied the axisymmetric buckling of radially loaded circular Mindlin plates with internal concentric ring support.

Mermertaş and Belek [24] studied the static and dynamic stability of variable thickness annular plates subject to periodic in-plane forces. For this purpose a sector finite element model with the wave propagation technique of cyclic symmetry is developed.

Teng and Rotter [25] studied the problem of elastic unstiffened thin cylinders with axisymmetric imperfections.

Rao and Ramanjaneyulu [26] presented the stability analysis of natural draught cooling tower shell subjected to non axisymmetric wind pressure carried out using finite ring elements. The finite element method is based on the development of a geometric stiffness matrix consistent with the elastic stiffness matrix of the element. The most suitable element for the plates of arbitrary configuration is the triangular one. The minimum number of degrees of freedom at each node being three, this method leads to solution of a large eigenvalue problem for the total structure which is time consuming and uneconomical.

Sato [27] designed a set of partial differential equations to enable elastic buckling analysis of incomplete composite plates with regard to the thickness of a steel plate. The relationship of critical buckling loads among complete composite plates, incomplete composite plates and individual plates was analyzed.

Singh and Dey [28] studied the total potential energy of buckling of a plate with variable stiffness which has been discretized by the method of finite difference.

The type of element selected can greatly affect the efficiency and quality of the approximate solution obtained. Due to their distinct geometrical and structural form, shells of revolution with axisymmetric loading, boundary conditions and material disposition can be idealized as effectively one-dimensional problems and can be solved efficiently using finite element method.

2.2 Structural Shape Optimization

Structural shape optimization techniques based on the finite element method have been used for many years with some success in the design of structures and structural components. Shape optimization of structures modeled using two dimensional representations was first investigated by Zienkiewicz and Campbell [29]. Since then much work has been reported [30-35].

One of the earliest attempts at optimizing vibrating circular plates addressed the problem of maximizing the fundamental frequency of vibration for a given volume of material and was carried out by Olhoff [36]. The analysis was based upon classical thin plate theory.

In the 1970's Hamada [37] used bending shell theory and finite differences to obtain the optimum shape of some axisymmetric shells with stress minimization as an objective.

Boisserie and Glowinski [38] investigated the optimum structural design of thin axisymmetric shell structures using an optimal control approach with stress minimization as an objective and allowing the thickness to be varied.

Plaut et al. [35] optimized the structural forms of thin shallow, elastic shells with a given circular boundary. Several objectives were considered such as maximizing the fundamental frequency, critical load and enclosed volume of the structure. The analysis was based on Marguerre's shallow shell theory.

Mota Soares et al. [39] considered optimal thickness variations for axisymmetnc shell structures with constraints on displacements, stresses and natural frequencies and with weight minimization as an objective. These studies involved rectilinear geometries (in the radial plane) and optimal thickness distributions which were piecewise constant with a stepped form. A two node linear element allowing for transverse shear deformation was used in their analysis.

Marcelin and Trompette [40] carried out shape optimization of axisymmetric shell structures using two or three node thin shell elements of constant thickness with the objectives of making the stress along a part of the boundary uniform and minimizing stress concentrations. However, their definition of structural geometries was restricted to straight or circular segments only.

The sensitivity analysis and optimal design for buckling load of thin multi-layered angle-ply composite structures has been studied by Mateus et al. [41]. The model was based on a plate-shell element with 18 degrees of freedom using the discrete Kirchhoff theory for bending effects. The objective of the optimization was the maximization of constrained or unconstrained buckling load parameter.

Levy and Spillers [41] studied the structural optimization problem of finding the optimal wall thickness of an axisymmetric cylindrical shell so as to maximize the buckling load when the volume of material is fixed. Levy and Ganz [43] developed the analysis of optimized plates for buckling. The Rayleigh-Ritz method was used to analyze variable thickness rectangular plates. The plate was optimized using variational calculus to obtain the optimality condition which states that the thickness is proportional to the strain energy density and a truncated Fourier series solution (one term) was used to obtain an optimal shape.

Lin and Liu [44] developed an optimization computer code automatic resizing systems applied for plate structures with buckling constraints.

Plaut and Johnson [35] optimized the structural forms of thin shallow, elastic shells with a given circular boundary. Several objectives were considered such as maximizing the fundamental frequency, critical load and enclosed volume of the structure. The analysis was based on Marguerre's shallow shell theory.

The membrane approximation was used to determine the shapes and thickness distributions for axisymmetric shell structures that can support specified loads with minimum material by Richmond and Azarkhin [45]. A Lagrange multiplier technique was employed. It resulted in Euler field equations and associated boundary conditions for the optimum shells. It also generated expressions for the multipliers directly in terms of the shell geometry. Specific solutions were obtained for the cases where the prescribed forces were uniform pressure, uniform vertical load and the weight of the shell itself. Both the Misses and the Tresca yield condition were used, and the optimum shells were shown to be in a state of yielding everywhere.

2.3 Remarks on Literature

The type of element selected can greatly affect the efficiency and quality of the approximate solution obtained. Due to their distinct geometrical and structural form, shells of revolution with axisymmetric loading, boundary conditions and material disposition can be idealized as effectively one-dimensional problems and can be solved efficiently using finite element method.

CHAPTER 3

ANALYSIS OF PLATES AND SHELLS OF REVOLUTION

3.1 Introduction

In the axisymmetric plate and shell problems, the cross-section of the shell does not change in the circumferential direction. If the material properties of the structures are also constant in the same direction, the analysis can be simplified by the combined use of finite elements and Fourier expansions to model the circumferential behavior.

The combination of finite element method and Fourier series was first applied by Grafton and Strome [46]. Considerable research work has subsequently been directed towards the improvement of solution accuracy and versatility of application as well as computational efficiency. A variety of elements have been proposed based on different structural theories (e.g. Kirchhoff-Love, Mindlin-Reissner shell theories) in order to achieve a more accurate prediction of structural response. See for example the texts by Zienkiewicz and Taylor [47] and Grould [48]. Hinton and co-workers [49-51] used linear, quadratic and cubic finite element based on Mindlin-Reissner assumptions for the free vibration and static analysis of curved and variable thickness, shell of revolutions.

3.2 Static Analysis

Shells of revolution with axisymmetric loading, boundary conditions and material disposition, due to their distinct geometrical and structural form can be idealised as effectively one-dimensional problems and can be solved efficiently on the basis of numerical procedures; FE method has been the most prominent in the analysis of shells of revolution. In the following sections basic formulations providing an accurate solutions for analysis of general shells of revolutions are presented.

3.2.1 Total potential energy

The finite element method is used to analyze axisymmetric shell structures in which the geometrical properties are invariant in a particular direction.

Consider the Mindlin-Reissner axisymmetric shell element shown in Figure 3.1. Displacement components u_ℓ, v_ℓ and w_ℓ are translation in the ℓ, η and n directions respectively. Note that η varies from an angle 0 to 2π along a curve of radius r. The displacement components u_ℓ and w_ℓ may be written in terms of global displacements u and w in the r and z directions as

$$\begin{aligned} u_\ell &= u\cos\alpha + w\sin\alpha \\ w_\ell &= -u\sin\alpha + w\cos\alpha \end{aligned} \tag{3.1}$$

where α is the angle between the r and ℓ axes; see Figure 3.1. The radius of curvature R may be obtained from the expression

$$\frac{d\alpha}{d\ell} = -\frac{1}{R} \tag{3.2}$$

Note that the displacement components v_ℓ and v coincide.

The total potential energy for a typical axisymmetric MR shell is given as

$$\begin{aligned} \Pi\,(u_\ell,\omega_\ell,\theta) &= \pi\int\Big([\boldsymbol{\varepsilon}_m]^T \mathbf{D}_m\boldsymbol{\varepsilon}_m + [\boldsymbol{\varepsilon}_b]^T \mathbf{D}_b\boldsymbol{\varepsilon}_b + [\boldsymbol{\varepsilon}_s]^T \mathbf{D}_s\boldsymbol{\varepsilon}_s \Big) r d\ell \\ &- 2\pi \int \omega_\ell q r d\ell - (M\overline{\theta} + N\overline{u_\ell} + Q\overline{\omega_\ell}) \end{aligned} \tag{3.3}$$

where the membrane strains are given by

$$\boldsymbol{\varepsilon}_m = [\varepsilon_\ell, \varepsilon_\psi]^T \tag{3.4}$$

in which the radial strain may be expressed in the terms of the local displacement as

$$\varepsilon_\ell = \frac{\partial u_\ell}{\partial \ell} + \frac{w_\ell}{R} \tag{3.5}$$

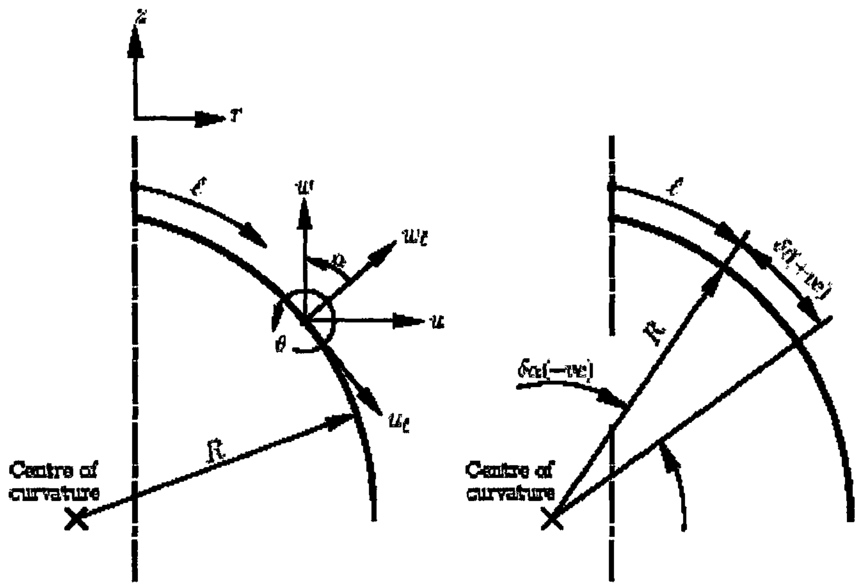

Figure 3.1 Definition of Mindlin-Reisner finite elements

or in the terms of global displacement as

$$\varepsilon_\ell = \frac{\partial u}{\partial \ell}\cos\alpha + \frac{\partial w}{\partial \ell}\sin\alpha$$

and the hoop or the circumferential strain is expressed as

$$\varepsilon_\psi = \frac{1}{r}\left(u_\ell \cos\alpha - w_\ell \sin\alpha\right) \tag{3.6}$$

or

$$\varepsilon_\psi = \frac{u}{r} \tag{3.7}$$

The bending strains or curvatures are given by

$$\varepsilon_b = [\chi_\ell, \chi_\psi]^T \tag{3.8}$$

where the radial curvutares

$$\chi_\ell = -\frac{d\theta}{d\ell} \tag{3.9}$$

and the hoop or circumferential curvature

$$\chi_\psi = -\frac{\theta\cos\alpha}{r} \tag{3.10}$$

The radial transverse shear strain is given by

$$\varepsilon_s = \frac{\partial \omega_\ell}{\partial \ell} - \theta - \frac{u_\ell}{R} \tag{3.11}$$

or

$$\varepsilon_s = -\theta - \frac{\partial u}{\partial \ell}\sin\alpha + \theta - \frac{\partial \omega}{\partial \ell}\cos\alpha \tag{3.12}$$

For an isotropic material of elastic modulus E, Poisson's ratio ν and thickness t, the matrix of membrane rigidities may be written as

$$\mathbf{D}_m = \frac{Et}{(1-\nu^2)}\begin{bmatrix} 1 & \nu \\ \nu & 1 \end{bmatrix} \tag{3.13}$$

the matrix of flexural (bending) rigidities has the form

$$\mathbf{D}_b = \frac{Et^3}{12(1-\nu^2)}\begin{bmatrix} 1 & \nu \\ \nu & 1 \end{bmatrix} \tag{3.14}$$

and the shear rigidity is given as

$$\mathbf{D}_s = \kappa \frac{Et}{2(1+\nu\ )} \tag{3.15}$$

where κ is the shear modification factor and is taken as 5/6 for an isotropic material. The loading in (3.3) consists of a distributed ring pressure loading q, as well as couples M, axial forces N or lateral forces Q applied along circumferential circle at $\ell = \bar{\ell}$. Note that $\bar{u}_\ell, \bar{\omega}_\ell$ and $\bar{\theta}$ are corresponding displacement and rotation values at $\ell = \bar{\ell}$.

3.2.2 Finite element idealization

Using n-noded, $C(0)$ elements,the global displacements parameters u ,ω and θ may be interpolated within each element by the expressions

$$u = \sum_{i=1}^{n} N_i\, u_i \ ; \quad \omega = \sum_{i=1}^{n} N_i\, u_i \ ; \quad \theta = \sum_{i=1}^{n} N_i\, \theta_i \tag{3.16}$$

where u_i, ω_i, θ_i are typical nodal degres of freedom and $N_i(\xi)$ is the shape function associated with node i, which for 2-noded linear elements has the form

$$N_1 = \frac{1}{2}(1-\xi) \ ; \quad N_2 = \frac{1}{2}(1+\xi) \tag{3.17}$$

for 3-noded, quadratic elements

$$N_1 = \frac{\xi}{2}(1+\xi) \ ; \quad N_2 = (1-\xi^2) \ ; \quad N_2 = \frac{\xi}{2}(1+\xi) \tag{3.18}$$

and for 4-noded cubic elements

$$N_1 = \frac{9}{16}(\frac{1}{9} - \xi^2)(\xi - 1) \quad ; \quad N_2 = \frac{27}{16}(1 - \xi^2)(\frac{1}{\xi} - \xi) \tag{3.19}$$

$$N_3 = \frac{27}{16}(1 - \xi^2)(\frac{1}{\xi} + \xi) \quad ; \quad N_4 = -\frac{9}{16}(\frac{1}{9} - \xi^2)(1 + \xi)$$

These elements are essentially iso parametric so that

$$r = \sum_{i=1}^{n} N_i \; r_i \; ; \quad z = \sum_{i=1}^{n} N_i \; z_i \; ; \quad t = \sum_{i=1}^{n} N_i \; t_i \tag{3.20}$$

where r_i, z_i and t_i are typical coordinates and thickness of node i respectively. Note also that Jacobian may be written as

$$J = \frac{d\ell}{d\xi} = \left[\left(\frac{dr}{d\xi} \right)^2 + \left(\frac{dz}{d\xi} \right)^2 \right]^{1/2} ; \qquad d\ell = J d\xi \tag{3.21}$$

where

$$\frac{dr}{d\xi} = \sum_{i=1}^{n} \frac{dN_i}{d\xi} r_i \; ; \quad \frac{dz}{d\xi} = \sum_{i=1}^{n} \frac{dN_i}{d\xi} z_i \tag{3.22}$$

also it is possible to write that

$$\sin\alpha = \frac{dz}{d\xi}\frac{1}{J} \; ; \quad \cos\alpha = \frac{dx}{d\xi}\frac{1}{J} \tag{3.23}$$

and

$$\frac{dN_i}{d\ell} = \frac{dN_i}{d\xi}\frac{1}{J} \tag{3.24}$$

The membrane strains may then be written as

$$\boldsymbol{\varepsilon}_m = \sum_{i=1}^{n} \mathbf{B}^e_{mi} \mathbf{d}^e_i \tag{3.25}$$

where

$$\mathbf{B}^e_{mi} = \begin{bmatrix} (dN_i / d\ell)\cos\alpha & (dN_i / d\ell)\sin\alpha & 0 \\ N_i & 0 & 0 \\ & & \end{bmatrix} \tag{3.26}$$

and

$$\mathbf{d}^e_i = [u_i, \omega_i, \theta_i]^T \tag{3.27}$$

The flexural strain or curvatures can be written as

$$\boldsymbol{\varepsilon}_b = \sum_{i=1}^{n} \mathbf{B}_{bi}^{e} \mathbf{d}_i^{e} \tag{3.28}$$

where

$$\mathbf{B}_{bi}^{e} = \begin{bmatrix} 0 & 0 & -dN_i/d\ell) \\ 0 & 0 & -N_i \cos\alpha / r \end{bmatrix} \tag{3.29}$$

and the shear strains are approximated as

$$\boldsymbol{\varepsilon}_s = \sum_{i=1}^{n} \mathbf{B}_{si}^{e} \mathbf{d}_i^{e} \tag{3.30}$$

where

$$\mathbf{B}_{si}^{e} = \left(-(dN_i/d\ell)\sin\alpha \quad (dN_i/d\ell)\cos\alpha \quad -N_i\right) \tag{3.31}$$

thus, neglecting circumferential line loads and couples, the contribution to the total potential energy from element *e* may be expressed as

$$\mathbf{K}_{ij}^{e} = 2\pi \int_{-1}^{+1} \{\mathbf{B}_{mi}^{T}\mathbf{D}_m\mathbf{B}_{mj} + \mathbf{B}_{bi}^{T}\mathbf{D}_b\mathbf{B}_{bj} + \mathbf{B}_{si}^{T}\mathbf{D}_s\mathbf{B}_{sj}\} rJd\xi \tag{3.32}$$

and the consistent nodal force vector associated with node *i* is written as

$$\mathbf{f}_i^{e} = \begin{pmatrix} 2\pi \int_{-1}^{+1} N_i q \sin\alpha \, rJd\xi \\ 2\pi \int_{-1}^{+1} N_i q \cos\alpha \, rJd\xi \\ 0 \end{pmatrix} \tag{3.33}$$

3.3 Free Vibration Analysis

3.3.1 Virtual Work

In the absence of external loads and damping effects, the virtual work (or more precisely the virtual power) for a typical curved axisymmetric Mindlin-Reissner shell element *e* is given in terms of the global displacements *u, v, w* and the rotations ϕ and ψ of the mid-surface normal in the ℓn and ηn planes respectively by the expressions[10]

$$I_e = \int_0^{2\pi} \int_{\ell^e} \left(\delta\, \boldsymbol{\varepsilon}_m^T \mathbf{D}_m \boldsymbol{\varepsilon}_m + \delta\, \boldsymbol{\varepsilon}_b^T \mathbf{D}_b \boldsymbol{\varepsilon}_b + \delta\, \boldsymbol{\varepsilon}_s^T \mathbf{D}_s \boldsymbol{\varepsilon}_s + \delta\, \mathbf{u}^T \mathbf{P}\, \ddot{\mathbf{u}} \right) r\, d\ell\, d\eta \tag{3.36}$$

The membrane strains $\boldsymbol{\varepsilon}_m$, bending strains or curvatures $\boldsymbol{\varepsilon}_b$, the transverse shear strains $\boldsymbol{\varepsilon}_s$ and the matrices of elastic rigidities $\mathbf{D}_m$, $\mathbf{D}_b$ and $\mathbf{D}_s$ have the same meaning as in (3.4)-(3.15) for the finite elements with static analysis.

3.3.2 Finite Element Idealization:

Using n-noded, $C(0)$ elements, the global displacements and rotations may be interpolated within each element by the expressions (3.16) The membrane strains $\boldsymbol{\varepsilon}_m$, the flexural strain or curvatures $\boldsymbol{\varepsilon}_b$, the transverse shear strain $\boldsymbol{\varepsilon}_s$ may then be expressed as in (3.25)-(3.31).

When we list the nodal displacement and accelerations in vectors $\mathbf{d}$ and $\ddot{\mathbf{d}}$ respectively, then upon substitution of (3.24)-(3.32) into (3.3) for all the elements we obtain the expression

$$\delta\,\mathbf{d}\lfloor \mathbf{Kd} + \mathbf{M}\ddot{\mathbf{d}} \rfloor = 0 \tag{3.37}$$

where $\mathbf{K}$ and $\mathbf{M}$ are the global stiffness and mass matrices respectively contain submatrices contributed from each element e linking nodes i and j and harmonics p and q has the form. These submatrices have the form

$$[\mathbf{K}_{ij}^e]^{pq} = \int_0^{2\pi}\int_{-1}^{+1}\left([\mathbf{B}_{mi}^p]^T\mathbf{D}_m\mathbf{B}_{mj}^q + [\mathbf{B}_{bi}^p]^T\mathbf{D}_b\mathbf{B}_{bj}^q + [\mathbf{B}_{si}^p]^T\mathbf{D}_s\mathbf{B}_{sj}^q\right) rJd\xi\, d\eta \qquad (3.38).$$

and

$$[\mathbf{M}_{ij}^e]^{pq} = \int_0^{2\pi}\int_{-1}^{+1}\left([\mathbf{N}_i^p]^T\mathbf{P}_m\mathbf{N}_j^q\right) rJd\xi\, d\eta \tag{3.39}$$

where typically

$$\mathbf{N}_i^p = N_i\begin{pmatrix} C_p & 0 & 0 & 0 & 0 \\ 0 & S_p & 0 & 0 & 0 \\ 0 & 0 & C_p & 0 & 0 \\ 0 & 0 & 0 & C_p & 0 \\ 0 & 0 & 0 & 0 & S_p \end{pmatrix} \tag{3.40}$$

Note that, $[\mathbf{K}_{ij}^e]^{pq}$ and $[\mathbf{M}_{ij}^e]^{pq} = 0$ if $p \neq q$ because of the orthogonality conditions

$$\int_0^{2\pi}\sin(p\eta)\sin(q\eta)d\eta = \pi/2 \qquad \text{if } p = q$$

$$\int_0^{2\pi} \sin(p\eta)\sin(q\eta)d\eta = 0 \qquad \text{if } p \neq q \qquad (3.41)$$

$$\int_0^{2\pi} \cos(p\eta)\cos(q\eta)d\eta = \pi/2 \qquad \text{if } p = q$$

$$\int_0^{2\pi} \cos(p\eta)\cos(q\eta)d\eta = 0 \qquad \text{if } p \neq q \qquad (3.42)$$

The matrix $[\mathbf{M}^e_{ij}]^{pp} = 0$ is independent of the harmonic number p and therefore, the same matrix can be used for all the different harmonic equations, so that

$$[\mathbf{M}^e_{ij}]^{pp} = \pi \int_{-1}^{+1} \{[N_i]^T\} \ PN_j\} rJd\xi \qquad (3.43)$$

$\mathbf{N_i} = \mathbf{N}_i \mathbf{I}_5$ in which $\mathbf{I}_5$ is a 5 x 5 identity matrix. To avoid locking behaviour, reduced integration is adopted i.e. 1-, 2-, 3-point Gauss-Legendre quadrature is used for the 2-, 3-, and 4-noded elements respectively. Note also that since the rigidities $\mathbf{D}_m$, $\mathbf{D}_b$ and $\mathbf{D}_s$ depend on the thickness t and since t is interpolated within each element e from the nodal values t_i elements of variable thickness in the ξ-direction may be easily accommodated in the present formulation.

Since the discretised virtual power expression (3.33) must be true for any set of virtual displacements $\delta \mathbf{d}^p$, then by taking advantage of the orthogonality conditions (3.37) and (3.38) it may be rewritten in uncoupled form for each harmonic p as

$$\left|\mathbf{K}^{pp}\mathbf{d}^p + \mathbf{M}^{pp}\ddot{\mathbf{d}}^p\right| = 0 \qquad (3.44)$$

Note that when p = 0 we are solving for axisymmetric vibrations. The general solution of (3.44) is written as

$$\mathbf{d}^p = \bar{\mathbf{d}}^p e^{i\omega_p t} \qquad (3.45)$$

where $e^{i\omega_p t} = \cos(\omega_p t) + i\sin(\omega_p t)$ and ω_p and $\bar{\mathbf{d}}^p$ are the p^{th} natural frequency and vibration mode (eigenvector). Thus (3.37) may be rewritten in the standard eigenvalue form for each harmonic p as

$$(\mathbf{K}^{pp} + \omega_p^2 \mathbf{M}^{pp})\bar{\mathbf{d}}^p = 0 \qquad (3.46)$$

3.4 Buckling Analysis

3.4.1 Virtual power

In the absence of external loads and damping effects, the virtual work (or more precisely the virtual power) for a typical curved axisymmetric Mindlin-Reissner shell element e is given in terms of the global displacements u, v, w and the rotations ϕ and ψ of the mid-surface normal in the ℓn and ηn planes respectively by the expressions [10].

$$U^e = \frac{1}{2}\int_0^{2\pi}\int_{\ell^e}\left(\boldsymbol{\varepsilon}_m^T \mathbf{D}_m \boldsymbol{\varepsilon}_m + \boldsymbol{\varepsilon}_b^T \mathbf{D}_b \boldsymbol{\varepsilon}_b + \boldsymbol{\varepsilon}_s^T \mathbf{D}_s \boldsymbol{\varepsilon}_s\right) r\, d\ell\, d\eta \tag{3.47}$$

The membrane strains $\boldsymbol{\varepsilon}_m$, bending strains or curvatures $\boldsymbol{\varepsilon}_b$, the transverse shear strains $\boldsymbol{\varepsilon}_s$ and the matrices of elastic rigidities $\mathbf{D}_m$, $\mathbf{D}_b$ and $\mathbf{D}_s$ have the same meaning as in (3.4)-(3.15) for the finite elements with static analysis.

3.4.2 Potential energy of the applied inplane stresses

Buckling occurs when a structure converts inplane strain energy into strain energy of bending with no change in externally applied load. A critical condition, at which buckling impends, exist when it is possible that the deformation state may change slightly in a way that makes the loss in inplane strain energy numerically equal to the gain in bending strain energy. In a thin-walled structure such as a shell of revolution, inplane stiffness is typically orders of magnitude greater than bending stiffness. Accordingly, small inplane deformations can store a large amount of strain energy, but comparatively large lateral deflections and cross-section rotations are needed to absorb this energy in bending deformations.

The potential energy of the applied inplane stresses $\sigma_\ell^0, \sigma_\eta^0$ and $\tau_{\ell\eta}^0$ arises from the action of the applied stresses on the corresponding second order strains $\varepsilon_\ell^{nl}, \varepsilon_\eta^{nl}, \gamma_{\ell\eta}^{nl}$ are given in [51] The potential energy of the shell of volume V is

$$V_g = \int_V \left(\sigma_\ell^0 \varepsilon_\ell^{nl} + \sigma_\eta^0 \varepsilon_\eta^{nl} + \tau_{\ell\eta}^0 \gamma_{\ell\eta}^{nl}\right) dV \tag{3.48}$$

where

$$\varepsilon_\ell^{nl} = \frac{1}{2}\left[\left(\frac{\partial u}{\partial \ell} + z\frac{\partial \psi_\ell}{\partial \ell}\right)^2 + \left(\frac{\partial v}{\partial \ell} + z\frac{\partial \psi_\eta}{\partial \ell}\right)^2 + \left(\frac{\partial w}{\partial \ell}\right)^2\right]$$

$$\varepsilon_\eta^{nl} = \frac{1}{2}\left[\left(\left(\frac{\partial u}{\partial \eta} + z\frac{\partial \psi_\ell}{\partial \eta}\right)\frac{1}{r} - \frac{v}{r}\right)^2 + \left(\frac{u}{r} + \frac{1}{r}\left(\frac{\partial v}{\partial \eta} + z\frac{\partial \psi_\eta}{\partial \eta}\right)\right)^2 + \left(\frac{1}{r}\frac{\partial w}{\partial \eta}\right)^2\right] \quad (3.49)$$

and

$$V_g = \frac{1}{2}\int_0^{2\pi}\int_{\ell^e}\sigma_\ell^0 t\left[\left(\frac{\partial u}{\partial \ell}\right)^2 + \left(\frac{\partial v}{\partial \ell}\right)^2 + \left(\frac{\partial w}{\partial \ell}\right)^2\right] + \sigma_\eta^0 t\left[\left(\frac{u}{r}\right)^2 + \left(\frac{1}{r}\frac{\partial u}{\partial \eta}\right) - \left(\frac{u}{v}\right)^2 + \left(\frac{1}{r}\frac{\partial v}{\partial \eta}\right) + \left(\frac{1}{r}\frac{\partial w}{\partial \eta}\right)^2\right]$$

$$+ \sigma_\ell^0\frac{t^3}{12}\left[\left(\frac{\partial \psi_\ell}{\partial \ell}\right)^2 + \left(\frac{\partial \psi_\eta}{\partial \ell}\right)^2\right]$$

$$+ \sigma_\eta^0\left[t\left(\frac{\psi_\ell}{r}\right)^2 + \frac{t^3}{12}\left(\frac{1}{r}\frac{\partial \psi_\ell}{\partial \eta}\right)^2 - t\left(\frac{\psi_\eta}{\ell}\right)^2 + \frac{t^3}{12}\left(\frac{1}{r}\frac{\partial \psi_\eta}{\partial \eta}\right)^2\right] r\,d\ell\,d\eta \quad (3.50)$$

3.4.3 Finite element idealization-Geometric stiffness matrix

Using n-noded, $C(0)$ elements, the global displacements and rotations may be interpolated within each element by the expressions (3.16) The membrane strains $\boldsymbol{\varepsilon}_m$, the flexural strain or curvatures $\boldsymbol{\varepsilon}_b$, the transverse shear strain $\boldsymbol{\varepsilon}_s$ may then be expressed as in (3.25)-(3.31).

We can now evaluate the geometric stiffness matrix $\mathbf{K}_\sigma^e$ associated with the potential energy V^e of the applied inplane stresses σ_ℓ^0 and σ_η^0 which can be expressed as

$$V^e = \frac{1}{2}\sum_{p=p_1}^{p_2}\sum_{q=q_1}^{q_2}\sum_{i=1}^{n}\sum_{j=1}^{n}\mathbf{d}_i^p[\mathbf{K}_{\sigma ij}^e]^{pq}\,\mathbf{d}_j^q \quad (3.51)$$

where a typical submatrix of $\mathbf{K}_\sigma^e$ of element e linking nodes i and j, harmonics p and q has the form

$$[\mathbf{K}_{\sigma ij}^e]^{pq} = \int_0^\beta\int_{-1}^{+1} t\left([\mathbf{S}_{ui}^p]^T\mathbf{H}\mathbf{S}_{uj}^q + [\mathbf{S}_{vi}^p]^T\mathbf{H}\mathbf{S}_{vj}^q + [\mathbf{S}_{wi}^p]^T\mathbf{H}\mathbf{S}_{wj}^q\right)$$

$$+\left([\mathbf{Q}_i^p]^T\mathbf{H}\mathbf{Q}_j^q + [\mathbf{R}_i^p]^T\mathbf{H}\mathbf{R}_j^q\right) r\,J d\xi\,d\eta \quad (3.52)$$

in which

$$\mathbf{S}_{ui}^{p}=\begin{bmatrix}(dN_i/d\ell)C_p & 0 & 0 & 0 & 0\\ (N_i/r)C_p+(pN_i/r)S_p & 0 & 0 & 0 & 0\end{bmatrix},$$

$$\mathbf{S}_{vi}^{p}=\begin{bmatrix}0 & (dN_i/d\ell)S_p & 0 & 0 & 0\\ 0 & -(N_i/r)S_p-(pN_i/r)S_p & 0 & 0 & 0\end{bmatrix},$$

$$\mathbf{S}_{wi}^{p}=\begin{bmatrix}0 & 0 & (dN_i/d\ell)C_p & 0 & 0\\ 0 & 0 & (pN_i/r)S_p & 0 & 0\end{bmatrix},$$

$$\mathbf{Q}_{i}^{p}=\begin{bmatrix}0 & 0 & 0 & (dN_i/d\ell)(t^3/12)C_p & 0\\ 0 & 0 & 0 & 0 & -(tN_i/r)C_p-(t^3pN_i/12r)C_p\end{bmatrix},$$

$$\mathbf{R}_{i}^{p}=\begin{bmatrix}0 & 0 & 0 & 0 & (t^3/12)(dN_i/d\ell)S_p\\ 0 & 0 & 0 & (tN_i/r)C_p+(t^3pN_i/12r)S_p & 0\end{bmatrix},$$

and

$$\mathbf{H}=\begin{bmatrix}\sigma_\ell^0 & 0\\ 0 & \sigma_\eta^0\end{bmatrix}.$$

Note that, $[\mathbf{K}_{ij}^{e}]^{pq}$ and $[\mathbf{K}_{\sigma ij}^{e}]^{pq}=0$ if $p\neq q$ because of the orthogonality conditions

$$\int_0^b \sin(p\pi\eta/b)\sin(q\pi\eta/b)d\eta=b/2 \qquad \text{if } p=q$$

$$\int_0^b \sin(p\pi\eta/b)\sin(q\pi\eta/b)d\eta=0 \qquad \text{if } p\neq q$$

$$\int_0^b \cos(p\pi\eta/b)\cos(q\pi\eta/b)d\eta=b/2 \qquad \text{if } p=q$$

$$\int_0^b \cos(p\pi\eta/b)\cos(q\pi\eta/b)d\eta=0 \qquad \text{if } p\neq q \tag{3.53}$$

To avoid locking behavior, reduced integration may be adopted, i.e. 1-, 2-, 3-point Gauss-Legendre quadrature is used for the 2-, 3- and 4-noded elements respectively. Note also that since the rigidities $\mathbf{D}_m,\mathbf{D}_b$ and $\mathbf{D}_s$ all depend on t and since t is interpolated within each element e from the nodal values t_i, elements of variable thickness in the transverse direction may be easily accommodated in the present formulation.

Nothing the orthogonality relation (4.37), on assembly of the contributions to the total potential energy $U+V$ from all of the elements and subsequent minimization with respect to the nodal values the following eigenvalue expression is obtained for each harmonic p

$$[\mathbf{K}^{pp} + \lambda^p \mathbf{K}_\sigma^{pp}]\bar{\mathbf{d}}^p = \mathbf{0} \tag{3.54}$$

where λ^p is the load factor by which the inplane stress σ_ξ^0 and σ_η^0 are multiplied to produce instability and $\bar{\mathbf{d}}^p$ is the associated buckling mode. In the present studies the eigenvalues are evaluated using the subspace iteration algorithm [53].

CHAPTER 4

ANALYSIS EXAMPLES

4.1 Introduction

In this chapter a series of static, free vibration and buckling examples will be analyzed respectively and then results will be compared with related references.

4.2 Static Analysis Examples

4.2.1 Clamped circular plate

In this example, a clamped circular plate shown in Figure 4.1 which is subjected to uniformly distributed load is to be statically analyzed. The plate that has radius of 10 in. (r=10 in), thickness of 0.1 in and is subjected to a distributed load of 1 lb/in² (p=1 lb/in²). The material properties used in static analysis are assumed as, elastic modulus E=1x10^7 lb/in² with Poisson's ratio ν=0.3

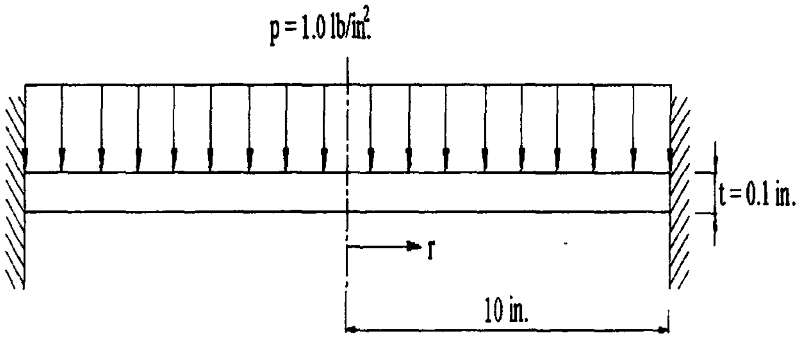

***Figure 4.1** Clamped circular plate under uniform load*

Discussion of results:

In this example for clamped circular plate static vibration analysis is carried out by Finite Element method using 16 linear, 14 quadratic, and 14 cubic elements. The results are tabulated in Table 4.1 for maximum values of deflection and bending moments. When the results are compared with Timoshenko and Woinowsk-Kreiger [54], close agreement can be observed for all the elements.

***Table 4.1** Values of deflection and stress resultants at the centre of a clamped circular plate*

ndof	element type	w_{max}	M_x	M_y
16	linear	0.171475	8.2344	8.3455
	quadratic	0.170707	8.1830	8.1555
	cubic	0.170703	8.1250	8.1250
28	linear	0.170939	8.1712	8.2062
	quadratic	0.170704	8.1775	8.1349
	cubic	0.170703	8.1250	8.1250
52	linear	0.170769	8.1421	8.1517
	quadratic	0.170703	8.1402	8.1279
	cubic	0.170703	8.1250	8.1250
exact	Ref [54]	0.170625	8.1250	8.1250

4.2.2 Spherical dome under uniform pressure

In this example, a clamped dome under uniform pressure shown in Figure 4.2 is statically analyzed. The dome that has radius of 90 in (r=90 in), thickness of 3 in and is subjected to a uniform load of 1 lb/in² (p=1 lb/in²). The material properties used in static analysis are assumed as elastic modulus E=2.0x10^6 lb/in² with Poisson's ratio ν=1/6.

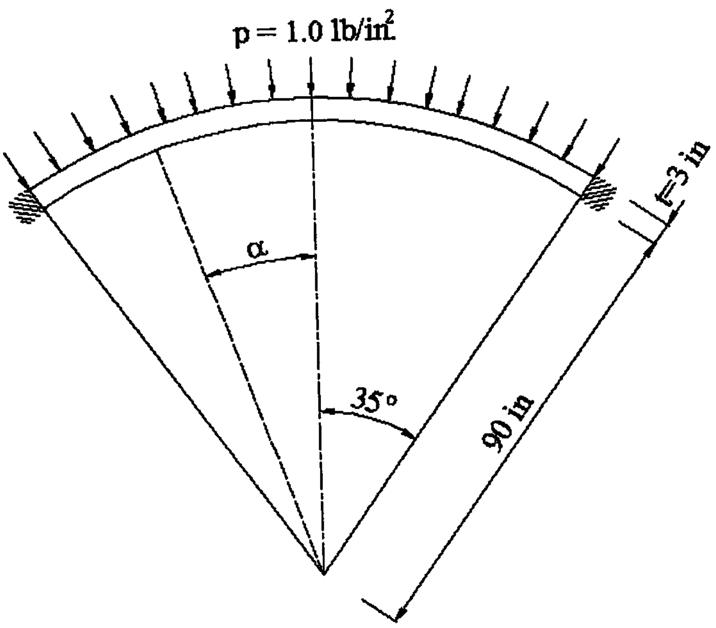

Figure 4.2 Spherical dome under uniform pressure

Discussion of results:

At the present study, spherical dome is analyzed by using linear, quadratic and cubic elements; the results are compared with the thin plate solutions reference [54] in Table 4.2. It can be clearly observed that the higher order element used the closer results acquired.

Table 4.2 Values of deflections and stress resultants of spherical dome

element type	w_{max} (in.)	N_ψ (lbs./in.) at $\alpha = 0^0$	M_ℓ (lbs.in./in.) at $\alpha = 35^0$
linear	0.82650	47.80	29.50
quadratic	0.81180	47.31	35.35
cubic	0.81190	47.30	36.38
exact		47.40	36.80

4.2.3 Toroidal shell under internal pressure

In this example, a toroidal shell which is under internal pressure is to be statically analyzed. The toroidal shell is formed by rotation of a circle about vertical axis for the given radius in Figure 4.3. The shell that has radius of 10 in, thickness of 0.1 in (t=0.1 in) and it has the pressure intensity of 1 lb/in² (p=1 lb/in²). The material properties used in static analysis are assumed as elastic modulus $E=10^7$ lb/in² with Poisson's ratio ν=0.3

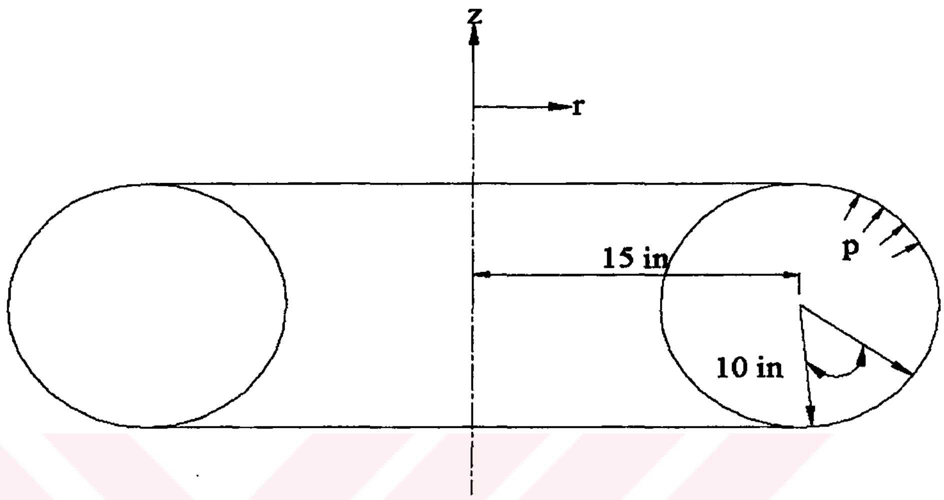

Figure 4.3 *Toroidal shell under internal pressure*

Discussion of results:

Static analysis of toroidal shell is carried out by using 31 linear, quadratic, cubic elements. The composition of strain energy is dominated by membrane energy with small contribution from bending and negligible from shear. The results are tabulated in the Table 4.3 for maximum values of deflection and bending.

Table 4.3 *Values of deflection and stress resultants of a toroidal shell under internal pressure*

Number of Element	Element type	Max. value of Membrane force	Max. value of Bending moment	Max. value of Shear force
31	cubic	2.0×10^1 lb/in.	-0.18 lb.in/in.	0.068 lb/in.

4.3 Free Vibration Analysis Examples

4.3.1 Hermetic can

A steel hermetic shown in Figure 4.4 has been analyzed for natural frequencies. The roller supported hermetic can that has the diameter of 228.6mm, length of 347mm and thickness of 2 mm. The material properties used in free vibration analysis are assumed: elastic modulus E= 207 Gpa, material density ρ=7800 kg/m^3 with Poisson's ratio ν=0.3

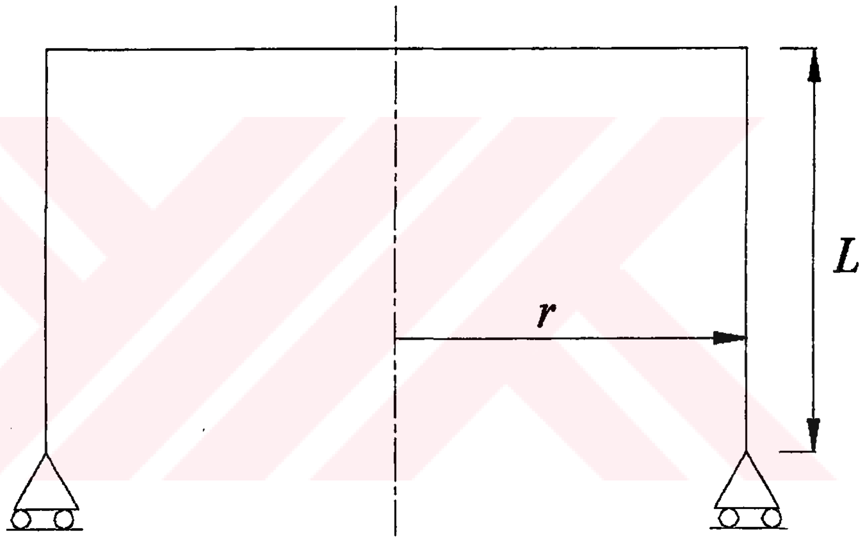

Figure 4.4 Geometry of a hermetic can

Discussion of results:

Free vibration analysis of steel Hermetic can is carried out by using 18 linear, quadratic, cubic elements. When the results are listed in Table 4.4 and compared with the results found by Tavakoli and Singh [55], close agreement can be observed at the first, second and the third harmonics at the first modes.

Table 4.4 *Natural frequencies (in hertz) of hermetic can.*

n(harmonic)	m(mode)	linear	quadratic	cubic	Ref [54]
0	1	354	353	353	360
	2	1486	1386	1385	-
	3	3727	3118	3104	-
1	1	753	735	734	620
	2	2361	2114	2111	-
	3	3216	3063	2991	-
2	1	1253	1205	1205	1200
	2	3107	2904	2897	-
	3	3434	3180	3178	-
3	1	1835	1761	1760	750
	2	2355	2335	2335	-
	3	4310	3834	3820	-

4.3.2 Hyperboloidal shell

Hyperboloidal shells, owing to their geometric properties, they are widely used in concrete structures. At the present study concrete hyperboloidal cooling tower in Figure 4.5 is analyzed. It is observed that any slight variations in geometry are leading large changes in natural frequency of the structure. Clamped concrete hyperboloidal cooling tower in accordance with geometry defining equations has been analyzed to verify its natural frequencies by using the geometric and material data which are parametrically defined as: a=25.603 m, d=82.194 m, height of the tower L=100.787 m, thickness of the shell t=0.127 m, elastic modulus E= 20.69 Gpa, material density ρ=2405 kg/m^3 and Poisson's ratio ν=0.15

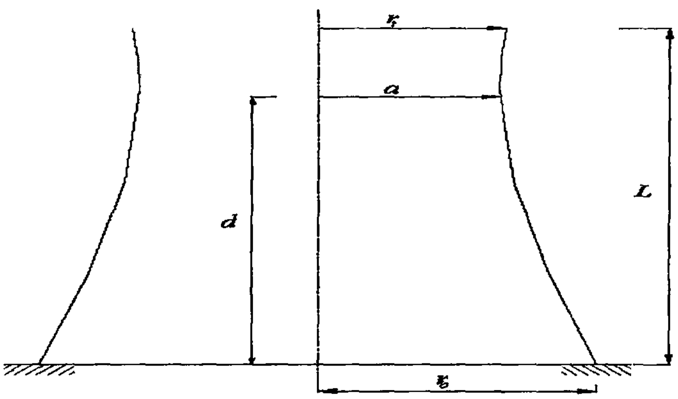

Figure 4.5 *Geometry of a hyperboloidal cooling tower*

Discussion of results:

At the present study, the results on the basis of thin shell theory integration technique with using finite element methods are acquired by using 68 cubic, quadratic, linear elements and then compared with the results of Carter et al. [56]. The results are tabulated for 6 harmonics and 3 modes of the structure. Close agreement is observed especially at the third and forth harmonics for linear element results, moreover, more approximate results are obtained at the first and second modes.

***Table 4.5** Natural frequencies (in hertz) of a hyperboloidal shell*

n	m	linear	quadratic	cubic	Ref [56]
0	1	7.7182	7.7184	7.7182	7.7494
	2	11.4598	11.4451	11.4441	11.4167
	3	12.0019	11.9845	11.9508	11.9023
1	1	3.2809	3.2807	3.2807	3.2884
	2	6.7753	6.7736	6.7736	6.7905
	3	10.5461	10.5419	10.5418	10.5207
2	1	1.7583	1.7581	1.7581	1.7654
	2	3.6575	3.6564	3.6564	3.6931
	3	7.0933	7.0888	7.0888	6.9562
3	1	1.3678	1.3671	1.3671	1.3749
	2	1.9699	1.9699	1.9701	1.9904
	3	4.5152	4.5142	4.5144	4.3254
4	1	1.2371	1.2366	1.2369	1.1808
	2	1.3525	1.3514	1.3513	1.4475
	3	2.9857	2.9891	2.9898	2.7777
5	1	1.0612	1.0601	1.0607	1.0348
	2	1.419	1.4187	1.4187	1.4293
	3	1.2396	2.2423	2.2434	2.0559

4.3.3 Cone-cylinder combination

An axisymmetric shell including cone-cylinder combination in Figure 4.6 has been studied in this example. Clamped cone-cylinder which has a radius of 114.3 mm (r=114.3mm), thickness of 2.03 mm *(t=2.03 mm)*, length of 171.5 mm (L=171.5mm) with the apex angle of 60 *(γ =60^0)*. The material properties used in free vibration analysis are elastic modulus E=207 Gpa, material density ρ=7800 kg/m^3 with Poisson's ratio ν=0.3

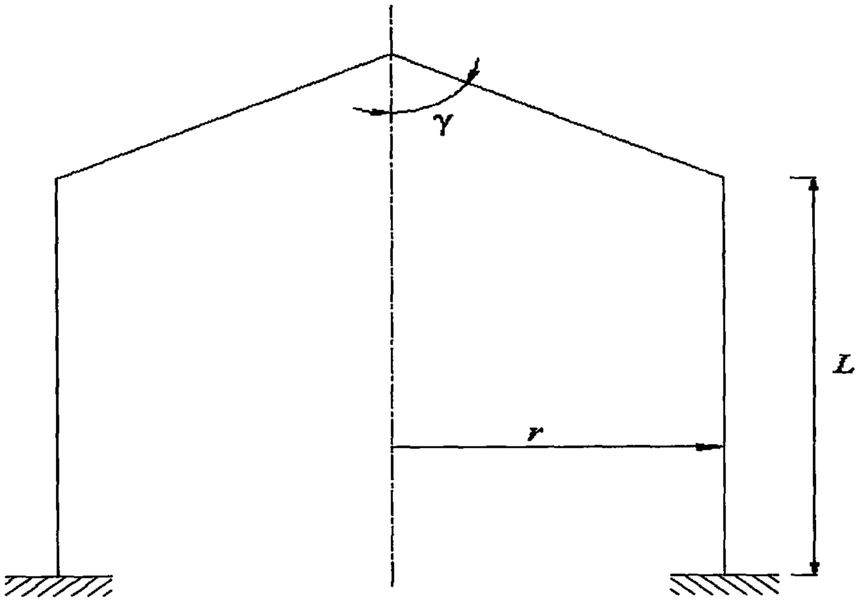

***Figure 4.6** Geometry of a cone-cylinder combination*

Discussion of results:

Steel cone-cylinder combination is analyzed by using 20 linear, quadratic and cubic elements. The results in Table 4.6 are compared with Tavakoli and Singh [57]; close agreement is obtained in quadratic and cubic element solutions for the second and third modes of the structure.

***Table 4.6** Natural frequencies (in hertz) of cone-cylinder combination*

n(harmonic)	m(mode)	linear	quadratic	cubic	Ref [57]
0	1	2522	2516	2516	2525
	2	5661	5578	5577	5585
	3	6527	6472	6471	6470
1	1	1965	1961	1961	1962
	2	3440	3421	3421	3432
	3	5401	5350	5350	5349
2	1	2091	2077	2077	2081
	2	3414	3356	3356	3357
	3	4689	4600	4599	4618
3	1	2134	2113	2113	2117
	2	2522	2465	2465	2465
	3	4754	4567	4563	4570

4.4 Buckling Analysis Examples

A set of simple supported and clamped circular Mindlin plates under uniaxial force N_x^0 is now considered to illustrate the convergence characteristics of various finite elements. The plates have thickness to radius t/R varying from 0.001 to 0.2. The results are represented in non-dimensional form using the buckling factor K which has form

$$K = \frac{(N_x^0)_{cr} R^2 t}{\pi^2 D} \tag{4.1}$$

where the flexural rigidity is written as

$$D = \frac{Et^3}{12(1-\nu^2)} \tag{4.2}$$

in which ν is the Poisson's ratio, $(N_x^0)_{cr}$ is the critical value of the inplane uniform radial force and E is the elastic modulus. Poisson's ratio ν is taken as 0.3.

4.4.1 Circular plates with one and two concentric ring support

Convergence studies have been carried out for simply supported and clamped circular Mindlin plates with one and two concentric ring support. The results obtained are presented in Table 4.7 and 4.8. The buckling factors decreases with increasing thickness-radius ratios due to the increasing deformation effect.

***Table 4.7** Buckling factors for radially loaded circular Mindlin plates with one concentric ring supports*

Edge Type	a_1/R	Buckling Factors, K		
		$t_1/R = 0.001$	$t_1/R = 0.1$	$t_1/R = 0.2$
Simply Supported	0.20	23.0558	21.0634	16.8599
	0.60	26.6238	24.3037	19.3700
	0.99	15.0755	9.4305	5.8869
Clamped	0.20	49.0235	41.9207	29.7262
	0.60	30.3772	26.7749	20.2215
	0.99	15.0997	14.1759	12.4473

Table 4.8 Buckling factors for radially loaded circular Mindlin plates with two concentric ring supports

Edge Type	a_1/R	Buckling Factors, K		
		$t_1/R = 0.001$	$t_1/R = 0.1$	$t_1/R = 0.2$
Simply Supported	0.10	57.4398	46.9221	31.2963
	0.20	68.1771	54.6792	35.3139
	0.30	74.0640	59.2473	38.0009
Clamped	0.20	90.9877	67.6890	39.7048
	0.60	95.5077	71.1997	41.8220
	0.99	83.3290	64.1121	39.4149

4.4.2 Cylindrical shells

A set of simple supported cylindrical shell under uniaxial force N_x^0 is now considered to illustrate the convergence characteristics of various finite elements. The results generated by the present approach given in Table 4.9 are also compared by Timoshenko and Gere [5]. Elastic modulus E is taken as *100*. Poisson's ratio ν is taken as *0.3*.

Table 4.9 Buckling factors for axially loaded cylindrical shell with simple support

L/R	t/R	Buckling Factors, K	
		Present Study	Timoshenko and Gere [5]
1	0.01	0.61851	0.60523
	0.10	5.61828	6.05223
10	0.01	0.60978	0.60523
	0.10	5.69640	6.05223
100	0.01	0.60976	0.60523
	0.10	5.69670	6.05223

CHAPTER 5

OPTIMIZATION ALGORITHM

5.1 Introduction

In structural design it is necessary to obtain an appropriate geometric shape for the structure so that it can carry the imposed loads safely and economically. This may be achieved by the use of structural shape optimization (SSO) procedures in which the shape or the thicknesses of the components of the structure are varied to achieve a specific objective satisfying certain constraints. Such procedures are iterative and involve several re-analyses before an optimum solution can be achieved. SSO tools can be developed by the efficient integration of structural shape definition procedures, automatic mesh generation structural analysis, sensitivity analysis and mathematical programming methods.

5.2 Mathematical Definition of Optimization Problem

The optimization problem may be summarized in the formal mathematical language of nonlinear programming as follows: Find the design vector s which *maximizes* (or minimizes) the objective fonction $F(\mathbf{s})$ *subject to* the behavioral constraints $g_j\,(\mathbf{s}) \leq 0$, equality constraints $h_k\,(\mathbf{s}) = 0$ and explicit geometric constraints $s_i^{l} \leq s_i^{l} \leq s_i^{u}$. The subscripts j, k and i denote the number of behavioral constraints, equality constraints and design variables respectively. The terms s_i^{l} and s_i^{u} refer to the specified lower and upper bounds on the design variables.

Table 5.1 summarizes the list of commonly used design variables, objective functions and inequality constraints in structural shape optimization. Note that, in general, the functions F, g_j and h_k may all be non-linear implicit function of the design variables **s**.

Table 5.1 Design variables, objective functions and constraints used in structural shape optimization

Design variables s

- Coordinates of key points s_k
- Thickness at key points t_k

Objective functions F(s)

- Weight
- Buckling load
- Strain energy
- Error energy
- Stress leveling
- Fundamental frequency

Constraint functions g(s)

- Stress constraint
- Displacement constraint
- Buckling loads
- Weight constraint
- Frequency constraint
- Surface constraint

In dynamic situation, the objective function is maximization of the fundamental frequency ω(**s**) or minimization of weight subject to frequency or weight constraints. However; in static situation minimization of SE, weight, error energy or stress leveling subject to stress, displacement and/or weight constraints. In addition, explicit geometrical constraints are imposed on the design variables to avoid impractical geometries. For example, a minimum element thickness is defined to avoid zero or 'negative' element thickness values. It is worth mentioning here that the objective function and the constraint hull may be non-convex and therefore local optima may exist.

5.3 Structural Shape Optimization Algorithm

The basic algorithm for structural shape optimization is given in Figure 5.1

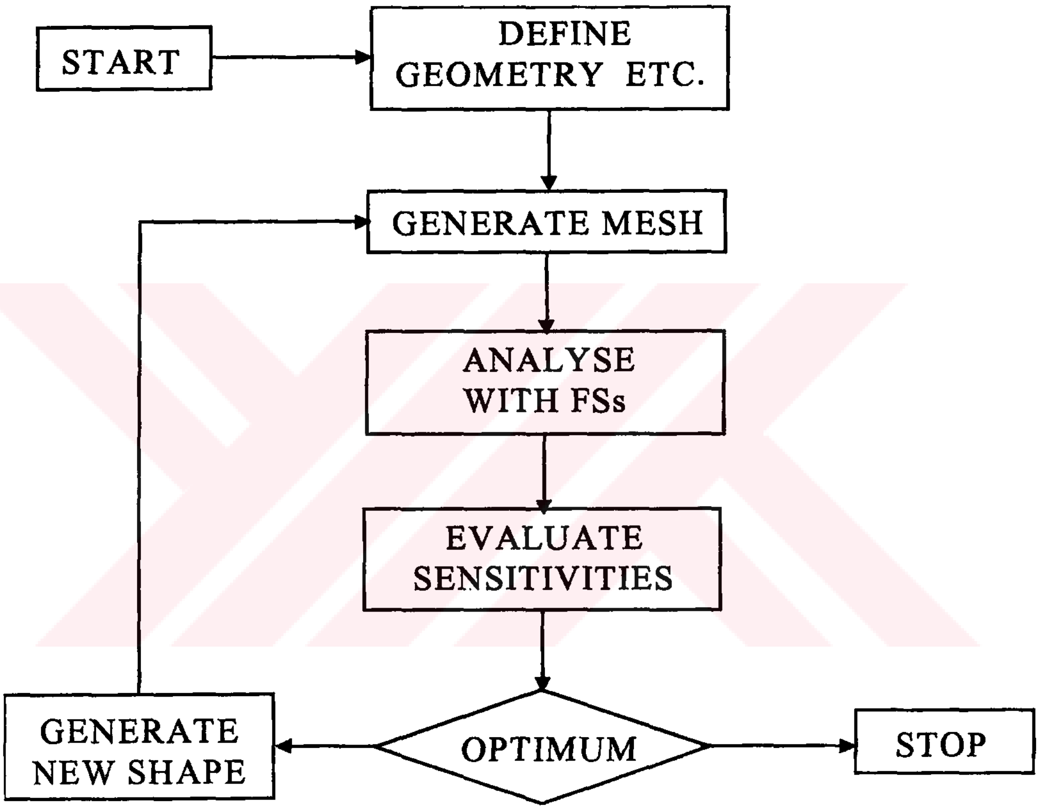

Figure 5.1 *Basic approach to structural shape optimization*

If we present an overview of a typical SSO procedure which is based on the following algorithm

1. Define the optimization problem including the objective function, constraints, design variables etc. The objective function and behavioral constraints are nonlinear implicit functions of the design variables.

2. Define the initial structural shape of the shell cross-section in terms of a set of design variables $s^{(1)} = [s_1^{(1)}, s_2^{(1)}, \ldots, s_n^{(1)}]^T$ which may include tbe coordinates and thickness of some specific points which define the cross-sectional geometry. (The superscript denotes the design number in other words the optimization iteration number).
3. Generate a mesh of suitable FE. This may be achieved with an automatic mesh generator for a prescribed mesh density. In this study, only uniform mesh densities are used.
4. Carry out a FE analysis for current design $s^{(c)}$ and evaluate the objective function and constraints. A feasible design variable vector $s^{(1)}$ usually used for initial designs but this is not always necessary.
5. In dynamic situation the sensitivities of the natural frequencies and the volume of the current design variables are evaluated. And in static situation the sensitivities of the SE, displacements and stress resultants of the current design to small changes in the design variables are evaluated. Methods for evaluating the sensitivities may be semi analytical or can be based on finite differences. In the present work, both methods are used.
6. Modify the current design and evaluate the design changes $\Delta s^{(c)}$ using the Method of Moving Asymptotes (MMA), Sequential Quadratic Programming (SQP), DOT.
7. Check the new design changes $\Delta s^{(c)}$. If the design changes $\Delta s^{(c)}$ are non-zero then update the design vector to

$$\Delta s^{(c+1)} = s^{(c)} + \Delta s^{(c)} \tag{5.1}$$

And continue the optimization process from step 3. Otherwise stop.

5.4 Geometry Definition

5.4.1 Structural shape definition

The definition and control of the geometric model of the structure to be optimized is a complex task. The shapes of structural domains encountered in practice are so arbitrary and complex that it is essential that they should be presented in a convenient way using computer aided design (CAD) tools, such as parametric cubic spline [24,25]

For the shake of convenience we have adopted certain standard terms for the representation of the shape of the structure which will be referred too frequently. The cross section of typical shells and folded plate structures are shown in Figure 5.2. They are formed by either a single or an assembly of segments. Each segment is a cubic spline curve passing through certain *key points* all of which lie on the midsurface of the structure cross-section. Some key points are common to different segments at their points of intersection. To represent a straight line the analysts have to provide a *minimum* of two key points lying on the segment and three points to represent a curved line.

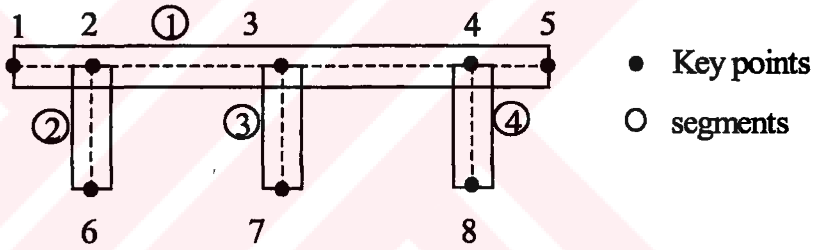

Figure 5.2 *Geometric representation of plate*

Another important aspect in shape optimization is the *number of key points* used to define the shape of the structure. For axisymmetric shells, the more key points used to better the representation of the middle surface of the shell. However, it should be noted that in SSO procedures increasing the number of key points leads to an increase in the number of design variables and is likely to lead to greater computational expense.

Sometimes for practical reasons and computational efficiency it is necessary to link the design variables at two or more key points. By judicious linking of design variables, the length of a segment can be treated as a design variable and symmetry of shape can be easily achieved; consequently, the number of design variables is considerably reduced.

5.4.2 Structural thickness definition

The thickness of the shell is specified at some or all of the key points of the structure and then interpolated using cubic splines or lower order functions and this results in smooth shell shapes.

Allowing only uniform thickness variations in SSO can over constrain the optimization process and does not give the greatest opportunity for objective function improvement. However, the use of *quartic* (or higher) thickness variation leads to excessive and impractical oscillations in the thickness distribution.

5.5 Mesh Generation

The next step is to generate a suitable FE mesh. This may be achieved with an automatic mesh generator for a prescribed mesh density. Mesh generation should be robust, versatile, and efficient. Here, we use a mesh generator which incorporates a remeshing facility to allow for the possibility of refinement. It also allows for a significant variation in mesh spacing throughout the region of interest. The mesh generator can generate meshes of two three and four noded elements and strips. Moreover, the shell thickness is also intepolate from the key points to the nodal points using cubic splines.

To control the spatial distribution of element sizes or mesh density throughout the domain, it is convenient to specify the mesh density at a sequence of points in the structure. Figure 5.3 shows a mesh of plates.

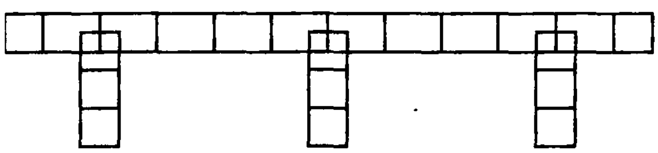

***Figure 5.3** Mesh representation of plates*

The mesh density is a piecewise linear function of the values of mesh size δ at some points along the midsurface of the structure. At the initial stages of the analysis, mesh density values given at the two end points of each segment will be sufficient if only a uniform or a linearly varying mesh density is required [25].

5.6 Structural Analysis

The efficiency of a method of optimum design is based on the computational time required in the process. Since most of the numerical optimization methods are iterative, the number of structural analyses required to complete the optimum solution is large. To reduce the computational efforts the efficient and inexpensive structural analysis method should be used.

To achieve an efficient method of optimum design of shell of revolutions with buckling constraints, finite element method can be employed in the process. Shells of revolution with axisymmetric loading, boundary conditions and material disposition can be idealized as effectively one-dimensional problems and can be solved efficiently using computer based numerical procedures. Detail of analysis of shells of revolution is presented in Chapter 3

5.7 Sensitivity Analysis

The sensitivities provide the mathematical programming algorithm with search directions for optimum solutions. Having completed the FE analysis, we now evaluate the sensitivities of the current design to small changes in the design variables. We calculate the sensitivities of items such as buckling load based on finite differences.

Sensitivity analysis consists of the systematic calculation of the derivatives of the response of the FE model with respect to parameters characterizing the model i.e. the design variables which may be length, thickness or shape. Finite element structural analysis programs are used to calculate the response quantities such as displacements, stresses, buckling loads etc. The first partial derivatives of the structural response quantities with respect to the shape (or other) variables provide the essential information required to couple mathematical programming methods and structural analysis procedures.

5.7.1 Derivative of displacements and stress resultants:

To get $\partial \mathbf{d} / \partial s_i$ and $\partial \boldsymbol{\sigma} / \partial s_i$ global finite difference method is used and following expressions may be written

$$\frac{\partial \mathbf{d}}{\partial s_i} \approx \frac{\mathbf{d}(s_i + \Delta s_i) - \mathbf{d}(s_i)}{\Delta s_i} \tag{5.2}$$

$$\frac{\partial \boldsymbol{\sigma}}{\partial s_i} \approx \frac{\boldsymbol{\sigma}(s_i + \Delta s_i) - \boldsymbol{\sigma}(s_i)}{\Delta s_i} \tag{5.3}$$

where Δs_i is step size, $\mathbf{d}(s_i + \Delta s_i)$ is evaluated by solving

$$\mathbf{K}(s_i + \Delta s_i)\mathbf{d}(s_i + \Delta s_i) = \mathbf{f}(s_i + \Delta s_i) \tag{5.4}$$

and $\boldsymbol{\sigma}(s_i + \Delta s_i)$ is found from

$$\boldsymbol{\sigma}(s_i + \Delta s_i) = \mathbf{D}(s_i + \Delta s_i)\mathbf{B}(s_i + \Delta s_i)\mathbf{d}(s_i + \Delta s_i) \tag{5.5}$$

5.7.2 Derivative of natural frequencies:

The governing equations for dynamic situation may be written as

$$(\mathbf{K}^{pp} - \omega_p^2 \mathbf{M}^{pp})\bar{\mathbf{d}}_p = \mathbf{0} \tag{5.6}$$

where for the pth harmonic $\mathbf{K}^{pp}$ is the stiffness matrix, $\mathbf{M}^{pp}$ is the mass matrix, ω_p is the frequency and $\bar{\mathbf{d}}_p$ is the vibration mode shape which is normalized so that

$$\bar{\mathbf{d}}_p^T \mathbf{M} \bar{\mathbf{d}}_p = 1 \tag{5.7}$$

when the eigenvalues are distinct, the expression for the frequency derivative with respect to design variable s_i can be derived from (5.6) and (5.7) so that

$$\frac{\partial \omega_p}{\partial s_i} = \frac{1}{2\omega_p} \overline{\mathbf{d}}_p^T \left(\frac{\partial \mathbf{K}^{pp}}{\partial s_i} - \omega_p^2 \frac{\partial \mathbf{M}^{pp}}{\partial s_i}\right) \overline{\mathbf{d}}_p \tag{5.8}$$

The derivatives of the stiffness and mass matrices can easily be obtained by semi-analytical method. The derivatives are computed by re-calculating $\mathbf{K}^{pp}$ and $\mathbf{M}^{pp}$ for a small perturbation Δs_i of the design variable (coordinates or thicknesses). The derivatives of the stiffness and mass matrices with respect to the design variable s_i may then be written as

$$\frac{\partial \mathbf{K}^{pp}}{\partial s_i} \approx \frac{\mathbf{K}^{pp}(s_i + \Delta s_i) - \mathbf{K}^{pp}(s_i)}{\Delta s_i} \tag{5.9}$$

$$\frac{\partial \mathbf{M}^{pp}}{\partial s_i} \approx \frac{\mathbf{M}^{pp}(s_i + \Delta s_i) - \mathbf{M}^{pp}(s_i)}{\Delta s_i} \tag{5.10}$$

5.7.3 Derivative of buckling load

In the FE displacement approach the governing equations for buckling situation may be written as

$$[\mathbf{K}^{pp} + \lambda^p \mathbf{K}_\sigma^{pp}] \overline{\mathbf{d}}^p = 0 \tag{5.11}$$

where for the pth harmonic $\mathbf{K}^{pp}$ is the stiffness matrix, $\mathbf{K}_\sigma^{pp}$ is the load matrix, λ^p is the buckling factor and $\overline{\mathrm{d}}_p$ is the buckling mode shape which is normalized so that

$$\overline{\boldsymbol{d}}_p^T \mathbf{K}_\sigma^{pp} \overline{\boldsymbol{d}}_p = 1 \tag{5.12}$$

when the eigenvalues are distinct, the expression for the buckling derivative with respect to design variable s_i can be derived from (5.11) and (5.12) so that

$$\frac{\partial \lambda^p}{\partial s_i} = \overline{\mathbf{d}}_p^T \left(\frac{\partial \boldsymbol{K}^{pp}}{\partial s_i} - \lambda^p \frac{\partial \mathbf{K}_\sigma^{pp}}{\partial s_i}\right) \overline{\boldsymbol{d}}_p \tag{5.13}$$

The derivatives are computed by re-calculating $\mathbf{K}^{pp}$ and $\mathbf{K}_\sigma^{pp}$ for a small perturbation Δs_i of the design variable (coordinates or thicknesses). The derivatives of the stiffness and mass matrices with respect to the design variable s_i may then be written as

$$\frac{\partial \mathbf{K}^{pp}}{\partial s_i} \approx \frac{\mathbf{K}^{pp}(s_i + \Delta s_i) - \mathbf{K}^{pp}(s_i)}{\Delta s_i} \tag{5.14}$$

$$\frac{\partial \mathbf{K}_{\sigma}^{pp}}{\partial s_i} \approx \frac{\mathbf{K}_{\sigma}^{pp}(s_i + \Delta s_i) - \mathbf{K}_{\sigma}^{pp}(s_i)}{\Delta s_i} \tag{5.15}.$$

5.7.4 Derivative of volume:

The volume derivative is calculated using a forward finite difference approximation

$$\frac{\partial V}{\partial s_i} \approx \frac{V(s_i + \Delta s_i) - V(s_i)}{\Delta s_i} \tag{5.16}$$

where the volume V of the whole structure (or cross-sectional area of the structure may also be used) can be calculated by adding the volumes of numerically integrated.

5.8 Mathematical Programming

Using the information derived from the analysis and design sensitivities, mathematical programming methods such as Sequential Quadratic Programming (SQP) or the MMA are used to generate shapes with improved objective function values. In the present work only the MMA algorithm [26] is used. No effort has been made to study the mathematical programming methods used for SSO procedures and the MMA algorithm is used here essentially as a 'black box'.

CHAPTER 6

OPTIMIZATION EXAMPLES

6.1 Introduction

In this chapter a series of static, free vibration and buckling examples will be considered for shape and thickness optimization of axisymmetric plates and shells. The design variables are used to define the shape or the thickness variation or both.

6.2 Static Optimization Examples

6.2.1 Cylindrical tank under hydrostatic pressure

A cylindrical tank shown in Figure 6.1 which is subjected to hydrostatic pressure is to be statically analyzed and optimized to minimize the weight of the tank for distinct variations of thickness variables with the limit on the effective stress $\sigma_{eff.}$ = 2.6 Mpa. The tank that has radius of 20 m. (r=20 m) , thickness of 0.813 m (t=0.813 m) The material properties are assumed as elastic modulus E=28.0 GPa , weight per unit volume γ = 9.81 kN/m^3 with Poisson's ratio ν=1/6. The geometry and properties of the initial design are identical to those adopted by Mota Soares et al. [39]. The design variables are the thicknesses at the key points. The following cases are considered: as shown in Figure 6.2.

a) One segment and two key points

b) One segment and three key points

c) One segment and four key points

d) Two segments and three key points

e) Two segments and five key points.

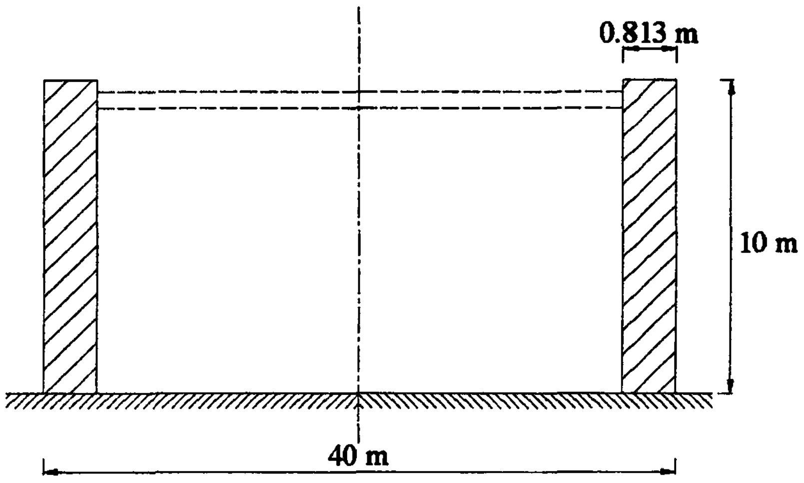

Figure 6.1 Cylindrical tank under hydrostatic pressure

Discussion of results:

At the present study, cylindrical tank is optimized for distinct thickness variations and according to optimal values for each case; the volume change is recorded. It is observed that remarkable volume reductions shown in Figure 6.2 are obtained when it is compared with initial volume. It can be observed that volume reduction is greater as more thickness variables are used.

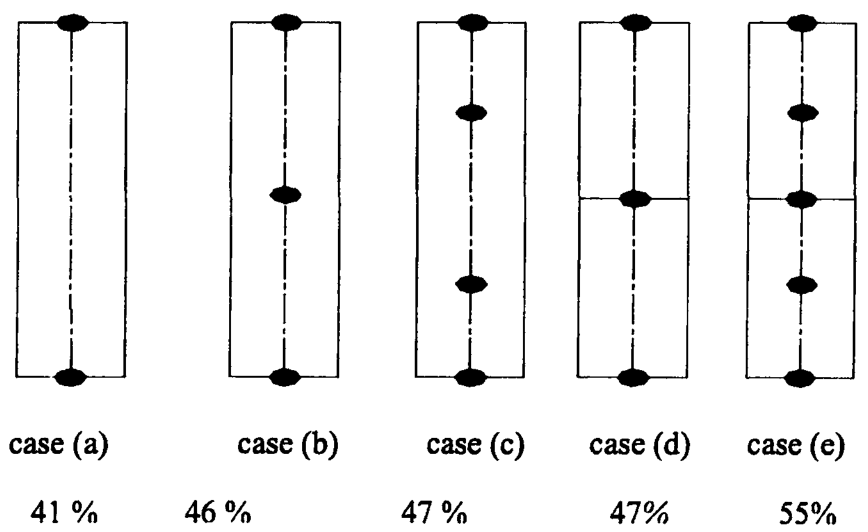

Figure 6.2 Locations of design variables for different cases and percentage volume reduction of cylindrical tank.

6.2.2 Umbrella-shaped concrete shell

In this example, an umbrella-shaped concrete shell presented by Imam [58] shown in Figure 6.3 is to be statically analyzed and optimized under gravity load only. To minimize the volume of the shell under the constraints on the allowable tensile stress σ_t =1.90 MPa, the allowable compressive stress σ_c =19.0 MPa, the allowable hoop stress σ_h =2.5 MPa. The shell that has radius of 2.0 m. (r=2.0 m), thickness of 0.050 m (t=0.050 m).The material properties are assumed as elastic modulus $E=28$ GPa , material density ρ=2360 kg/m^3 with Poisson's ratio ν=0.15. The design variables and shape variables are employed at the key points shown in Figure 6.4.

Several trials for design carried out to assume the apex angle. Trials are made to approximate the final design; the trials are supposed to converge the final design. Thickness and shape variables are designated for optimization at three key points as shown in Figure 6.4.

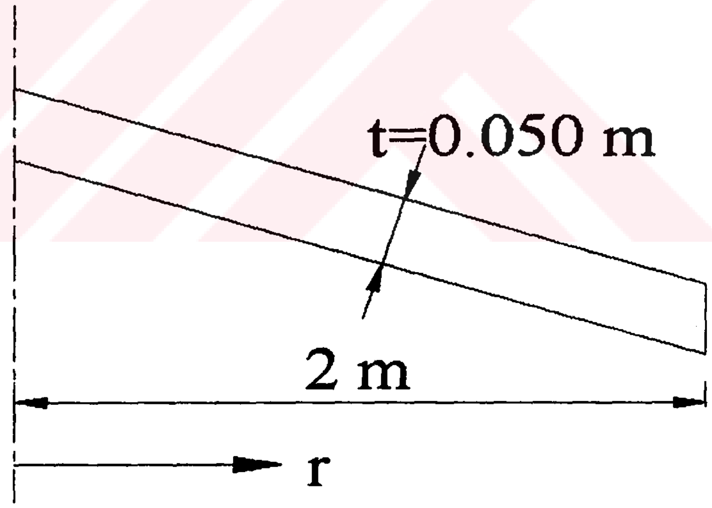

***Figure 6.3** Umbrella-shaped concrete shell.*

***Table 6.1** The results and percentage of reduction obtained for several trials for umbrella-shaped shell.[58]*

Trial No	Trial 1	Trial 2	Trial 3	Trial 4
Initial Mass(kg)	6298	9732	5303	4521
Final Mass(kg)	3565	3505	3763	3506
Reduction	43%	64%	29%	22%

Table 6.2 The optimized (final) results of present study and percentage of reduction obtained for several trials for umbrella-shaped concrete shell.

Trial No	Trial 1	Trial 2	Trial 3	Trial 4	Trial 5	Trial 6
Initial Mass(kg)	7024	6408	6767	6314	8885	8046
Final Mass(kg)	2159	2233	2043	2202	2370	2179
Reduction	69%	65%	70%	65%	73%	73%

Discussion of results:

At the present study, umbrella-shaped concrete shell is optimized for thickness and shape variations, the results of optimal design (final) and relevant volume reductions are listed in Table 6.2. When the results are compared with the results obtained by Imam [58] it can be observed that better volume reduction percentages acquired.

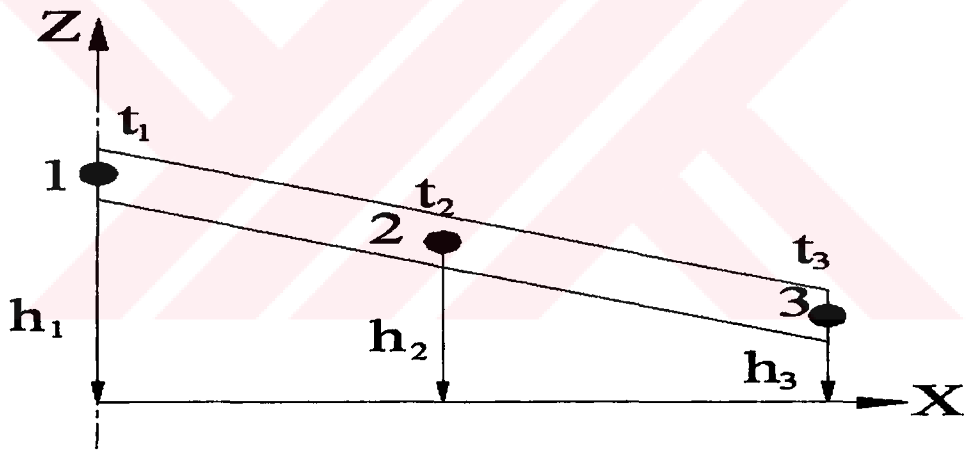

Figure 6.4 Umbrella-shaped concrete shell optimized for two segments three key points.

6.2.3 Clamped circular plate

In this example, a clamped circular plate which was presented by Mota Soares et al. [39] shown in Figure 6.5, which is subjected to uniformly distributed load is to be statically analyzed and optimized to minimize the volume of the plate under the constraints on the maximum displacement w_{max} = 5.5 mm and the equivalent stress σ_{eq} =73.5 MPa. The plate that has radius of 1.0 m. (r=1.0 m), thickness of 0.025 m (t=0.025 m) and is subjected to a distributed load of 0.0689 MPa (p=0.0689 MPa).

The material properties are assumed as elastic modulus $E=200$ GPa, material density ρ=7800 kg/m^3 with Poisson's ratio ν=0.3.

The design variables are the thicknesses at the key points. Five segments and six key points are used; thicknesses of five segments are design variables as shown in Figure 6.6.

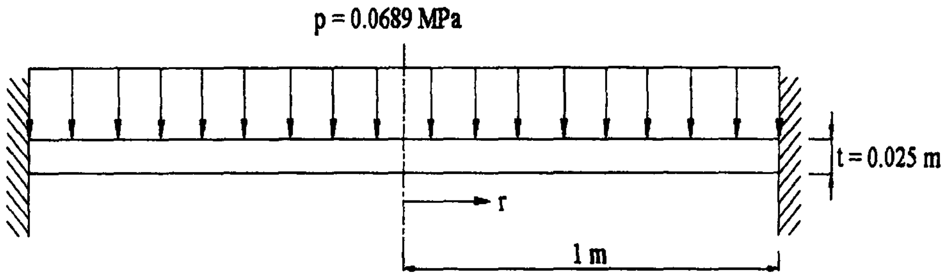

Figure 6.5 Clamped circular plate under uniform load

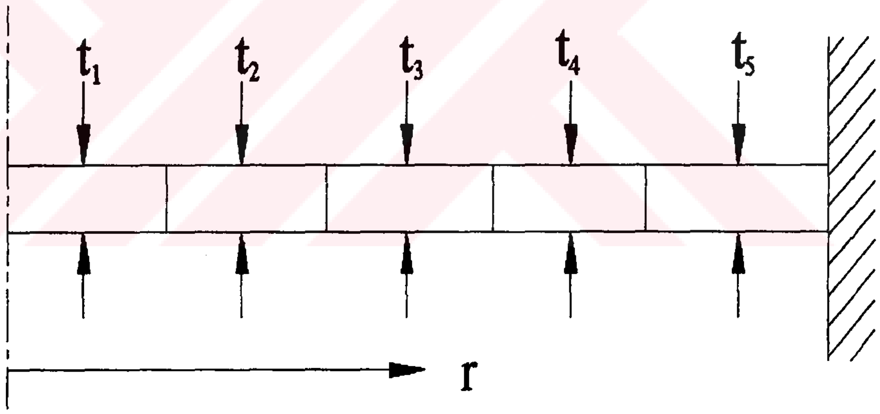

Figure 6.6 Clamped circular plate optimized for five segments six key points

Discussion of results:

At the present study, clamped circular plate is optimized for thickness variations ,the results of optimal design variables and relevant volume reductions are listed in Table 6.3. When the results are compared it is observed that minor volume reduction exists for different element types.

***Table 6.3** Optimal values of design variables and pertaining volume reduction percentages of clamped circular plate*

variations	Optimal design variables		
	linear	quadratic	cubic
t_1	25	25	25
t_2	22,19	25	25
t_3	13,96	20,82	20,94
t_4	17,05	16,24	16,23
t_5	25	25	25
	% volume reduction		
	19,08	13,14	13,06

Initial value of variables: 25 mm
Upper bound of variables: 25 mm
Lower bound of variables: 10 mm
Initial volume of the plate: 7.854×10^{-2} m^3

6.3 Free vibration optimization examples

6.3.1 Conical shell

In this example, optimization of clamped conical shell which was presented by Barbosa et al. [59] is dealt. The optimization is done in two stages. In the first stage volume is constrained to a constant value; in the second stage, the volume is constrained to remain unchanged. Three objective functions which considered for both cases are: (a) maximization of the fundamental axisymmetric frequency. (b) maximization of the lowest frequency (c) maximization of the sum of the five frequencies. The material properties used in the optimization process are assumed as elastic modulus E= 30 Gpa, Poisson's ratio ν=0.15, material density ρ=2410 kg/m^3. The initial geometry of the conical shell is as shown in the Figure 6.7. In the first stage of optimization, shape changes alone are considered; four key points and three straight segments are designated for geometrical definition of the conical shell. In the second stage optimization, the shape of the structure remains constant (and equal to the optimized shape of the first stage of the optimization); only thickness is allowed to change.

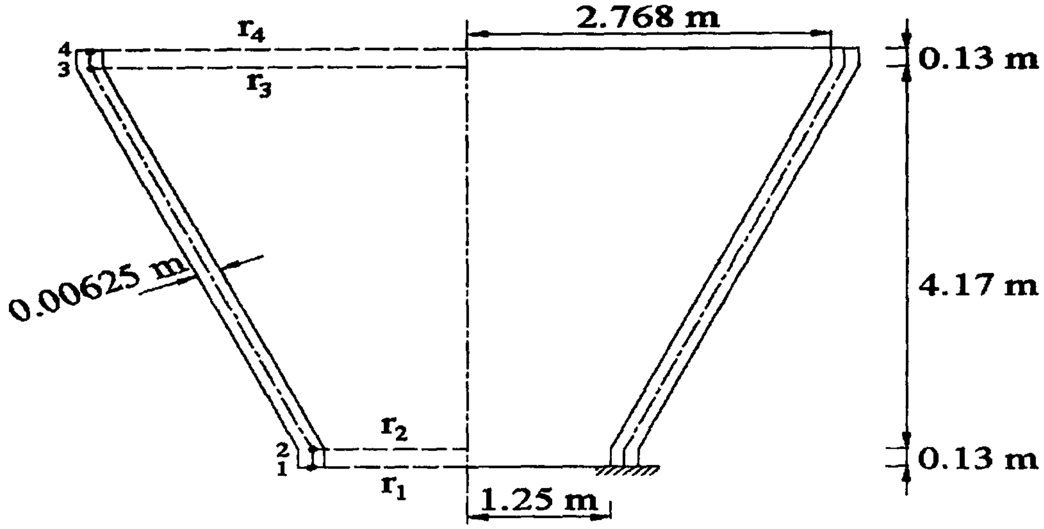

Figure 6.7 Conical shell-initial geometry (t=0.00625 m)

Table 6.4 Geometric limits on design variables of conical shell

stage	design variables			
	type	max	min	initial
1	s_1	4,0	1,0	1,250
	s_2	4,0	1,0	2,768
2	s_1	0,12	0,0000	0,0625
	s_2	0,12	0,0011	0,0625

Discussion of results:

(a) Maximization of the fundamental axisymmetric frequency:

At the first stage of optimization, the fundamental axisymmetric frequency of the shell increased from 862 to 1305 rad/sn in the Table 6.5. When compared with the values obtained by Barbosa et al. [59] the increase is from 866 to 1288 rad/sn so close agreement can be observed by comparison. At the second stage the optimized values of shape design values are designated as the initial shape values and then re-optimized for thickness variables that are listed in Table 6.6 and observed that the fundamental axisymmetric frequency increased from 1305 to 1809 rad/sn.

(b) Maximization of the lowest frequency:

At the first stage the lowest frequency increased from 107 to 244 rad/sn; At the second stage the lowest frequency increased to 310 rad/sn

(c) Maximization of the sum of the five frequencies:

The sum of the five frequencies for the first modes increased 1484 to 2767 rad/sn at the first stage and increased from 2767 to 3559 rad/sn at the second stage.

***Table 6.5** The results of conical shell for three distinct objective functions under three alternative constraints.*

n	m	initial	stage 1			stage 2		
			(a)	(b)	(c)	(a)	(b)	(c)
0	1	862	1305	1265	1298	1809	1516	1650
	2	1248	1799	1466		1918	1634	
	3	1404	1883	1586		2022	1785	
1	1	234	558	628	591	876	916	897
	2	956	1228	1172		1514	1388	
	3	1270	1632	1404		1799	1582	
2	1	113	265	302	282	460	501	477
	2	625	782	772		1013	982	
	3	1129	1317	1203		1482	1357	
3	1	107	242	244	243	295	310	290
	2	438	551	548		718	704	
	3	900	1013	960		1179	1109	
4	1	168	369	333	353	286	266	245
	2	405	525	506		597	560	
	3	772	864	821		987	924	

***Table 6.6** The values of design variables for conical shell.*

stage	opt. design variables			
	type	(a)	(b)	(c)
1	s_1	2.1202	2.6411	2.3334
	s_2	1.500	1.500	1.5
2	s_1	0.1137	0.113	0.0959
	s_2	0.0011	0.0011	0.0011

6.3.2 Circular plate

In this example, the optimization of circular plate is considered as once carried out by Olhoff [36] by maximizing the fundamental axisymmetric frequency of vibration for a given volume of material on the basis of classical thin plate theory. We now consider the optimization of some of these circular plates for our model under distinct support conditions which are (a) clamped edge conditions (b) simply supported edge condition and (c) clamped conditions at the centre of the plate. The material properties used in the optimization process are assumed as elastic modulus E= 30 Gpa, Poisson's ratio $\nu=0.3$, volume V=0.2.

Three different thickness variations are considered: 2 variables located at r=0.0 and r=1.0; 3 varaibles located at r=0.0, 0.5 and 1.0; 4 variables located at r=0.0, 0.33, 0.66 and 1.0

Discussion of results:

(a) Plate with clamped edges:

Optimum design variables and relevant optimum frequencies for the plate with clamped edges are given in Table 6.7. Optimum shapes are similar to the linear thickness variations obtained by Thambiratnam and Thevendran [60]. When the results of optimum frequencies for three thickness variations are 4.17, 4.33, 4.74 respectively .The four variable thickness variation result compares favorably with 4,91 obtained by Olhoff [36].

(b) Plate with simply supported edges:

The initial fundamental frequency of the plate with simply supported edges is equal to 1.56, and the optimal fundamental frequencies are equal to 1.75, 1.79, 1.80 for three thickness variations; The results are close to the value of 1.82 obtained by Olhoff [36]. The optimum values of design variables are given in Table 6.8

(c) Plate clamped at its centre:

The initial fundamental frequency of the plate with simply supported edges is equal to 1.17, and the optimal fundamental frequencies are equal to 4.13, 5.90, 5.60 for three thickness variations; the results are close to the value of 6.37 obtained by Olhoff [36]. The optimum values of design variables are given in Table 6.9

Table 6.7 *Circular plate with clamped boundary conditions: values of the optimal design variables.*

no of design variables	optimal values of design variables				Optimal fund. Frequency
	t_1	t_2	t_3	t_4	
2	0.00000	0.09549	-	-	4.17
3	0.00000	0.04005	0.10906	-	4.33
4	0,0000	0,0185	0,07266	0,09162	4.74

**Maximum and minimum bounds on the design variables are 0.12 and 0.00.*
**Initial values of design variables are all designated as 0.06366.*
**Initial fundamental frequency is 3.21*

Table 6.8 *Circular plate with simply supported boundary conditions: values of the optimal design variables*

no of design variables	optimal values of design variables				optimal fund. Frequency
	t_1	t_2	t_3	t_4	
2	0.13020	0.03039	-	-	1.75
3	0.08565	0.08829	0.01890	-	1.79
4	0.09782	0.09072	0.07395	0.01596	1.80

**Maximum and minimum bounds on the design variables are 0.14 and 0.00.*
**Initial values of design variables are all designated as 0.06366.*
**Initial fundamental frequency is 1.56*

Table 6.9 *Circular plate clamped at its centre: values of the optimal design variables*

no of design variables	optimal values of design variables				Optimal fund. Frequency
	t_1	t_2	t_3	t_4	
2	0.19098	0.00000	-	-	4.13
3	0.35000	0.09019	0.00000	-	5.90
4	0,3289	0,1565	0,0382	0,00001	5,60

**Maximum and minimum bounds on the design variables are 0.35 and 0.00.*
**Initial values of design variables are all designated as 0.06366.*
**Initial fundamental frequency is 1.17*

6.4 Buckling optimization examples

6.4.1 Axisymmetric plates

Axisymmetric plate is modeled using one segment and two, three, four, five key points with various combinations of boundary condition. Thickness design variables are the thickness of key points of plate.

The initial critical buckling load of the circular plate is equal to 1.490. The optimization is carried out for maximization of the critical buckling load. Constraints are volume and buckling load. The results generated by the present approach are given in Table 6.10 for simple support and Table 6.11 for clamped edges. The following material properties are assumed: Poisson's ratio $\nu = 0.3$, $t = 0.1$ and $P = 1kip$.

***Table 6.10** Simply supported circular plate: values of the optimal design variables and buckling ratio for* $t/R = 0.01$.

No of design Variables	optimal values of design variables					buckling ratio $R = K_{opt}/K_u$
	t_1	t_2	t_3	t_4	t_5	
2	0.12454	0.07546	-	-	-	1.0553
3	0.10330	0.11624	0.04256	-	-	1.1389
4	0.10411	0.11825	0.10600	0.02915		1.1421
5	0.10930	0.11647	0.11129	0.09565	0.02857	1.1534
Constraints: $t_{min} = 0.025$, $t_{max} = 0.3$ and $\lambda_1 \cdots, \lambda_{10} \geq 1.49$ Initial values: $\lambda_1 \cdots, \lambda_{10} = 1.490$ and $t_i = 0.1$						

***Table 6.11** Clamped circular plate: values of the optimal design variables and buckling ratio for* $t/R = 0.01$.

No of design Variables	optimal values of design variables					buckling ratio $R = K_{opt}/K_u$
	t_1	t_2	t_3	t_4	t_5	
2	0.03157	0.16843	-	-	-	1.3481
3	0.02500	0.10719	0.15095	-	-	1.3547
4	0.02500	0.08324	0.10312	0.21224		1.3804

5	0.02500	0.07128	0.09789	0.10346	0.25330	1.4093
Constraints: $t_{min} = 0.025$, $t_{max} = 0.3$ and $\lambda_1 \cdots, \lambda_{10} \geq 0.425$ Initial values: $\lambda_1 \cdots, \lambda_{10} = 0.425$ and $t_i = 0.1$						

CHAPTER 7

CONCLUSION AND FURTHER WORK

7.1 Conclusion

On the basis of mathematical programming techniques with a numerical structural analysis method, a general structural shape optimization algorithm method has been presented. Computational tools have been developed for geometric modeling, automatic mesh generation, FE analysis, behavior sensitivity analysis which has been successfully applied to the maximization of critical buckling load and natural frequency of the structure in addition to volume minimization of axisymmetric plates and shells under static situations. Several examples have been studied and used to test and to demonstrate the capabilities offered by these computational tools. The numerical results, compared with other studies, show the accuracy and performance of analysis methods.

7.1.1 Structural analysis

- Element types presented in the present work, which can perform well in *thick*, *thin* and *variable thickness* cases, have proved to be most appropriate for the analysis and optimization of shell structures due to their inexpensiveness, accuracy and reliability.
- The results obtained using FE analysis tools generally compare well with those obtained from other sources based on alternative formulations. The results

illustrate that the FE methods presented here can be used with confidence for the buckling analysis of axisymmetric plates and shells.

7.1.2 Structural optimization

- The integrated SSO algorithm described in this thesis is robust and reliable and provides and efficient way of finding optimum shapes for variable thickness axisymmetric plate and shell structures.
- The application of structural shape optimization in conjunction with FE analysis is an efficient and effective method, in particular for problems with a great number of design variables and a reasonable number of design constraints.
- Definition of the shape variables is crucial, i.e. the parameterization of the optimization model has to have as few degrees of freedom as possible to simplify the optimization task and as many degrees of freedom as necessary so that the problem is not over-constrained. The optimum solution obtained is only the optimum for this particular problem definition; in only very rare cases will it be the global optimum.
- Incorrectly formulated optimization problems may lead to designs which at best show very little reserve because of tight constraints margins and at worst are imperfection sensitive and fail prematurely. Also local optima may be produced which are long way from the global optimum. Consequently, care should be taken in the selection of appropriate design variables, the accurate representation of the boundary curves and the selection of the objective function and constraints.
- The more accurate the information given to the optimizer, the faster the convergence achieved. FE solutions in combination with the semi-analytical sensitivity method deliver more accurate function and derivative values.
- In certain special cases, we have demonstrated that the strain energy, volume and buckling load can be improved by as much as 50, 65 and 70 percent respectively using shape optimization.
- The introduction of thickness as well as shape variation leads to a further improvement in the objective function of the optimal structures.
- Some of the optimum shapes presented in this thesis are not practical and are included to show how shape and thickness changes can substantially alter the

values of objective function. However, manufacturing constraints etc. can be imposed to produce more practical optimum designs.

- The tools developed in the present work are useful creative design aids for structural engineers and could be used for teaching structural behavior to students, and assisting engineers in their quest for novel structural forms for shells and plates.
- Fully integrated design system can be developed by combining computer aided geometry modeling, mathematical programming methods, structural analysis, and behavior sensitivity analysis.

7.2 Further Work

Some suggestions exist for extending the various aspect of the present work can be summarized as follows:

7.2.1 Structural analysis

- The use of superstrips and the concept of repetitiveness of structure should be investigated to gain economy and accuracy in the analysis and optimization of prismatic plates and shells.
- The FE analysis code should extend to handle the buckling analysis of prismatic plates and shells curved planform.

7.2.2 Structural optimization

- The optimization of structures constructed from composite materials should be considered. In plates and shells, this would involve optimizing the fiber directions as well as the number and thickness of the plies.
- In SSO of structures analyzed by FE method, the use of other objective functions such as minimization of error energy, or stress leveling (where a uniform stress distribution is desired) should be investigated. Further, multi-objective problems should be considered in which there are several objective functions to be minimized and/or maximized. The user friendliness of the SSO algorithm should

be investigated by developing a modern user interface. It would also be of interest to integrate the present SSO algorithm with a standard CAD system.

7.2.3 Other subjects

- There is a clear need of benchmarks in all of the fields involved in optimization: FE analysis, sensitivity analysis and optimization.
- Topology optimization based on homogenization, evolution method and optimality criteria should be studied.
- Further areas of interest, such as multidisciplinary optimization including coupled problems (solid/fluid/soil/rock interaction) and thermal problems should be studied.

LIST OF REFERENCES

[1.] Özakça, M., *Analysis and Optimal Design of Structures with Adaptivity*, Ph. D. thesis, Department of Civil Engineering University College of Swansea, U.K., 1993

[2.] Billington, D.B., *Thin shell structures*, Newyork: McGraw-Hill Book Co., 1965.

[3.] Gould, P.L., *Static analysis of shells*, Toronto, Canada: Lexington Books, 1977.

[4.] Zingoni, A., *Shell structures in civil and mechanical engineering*, London: Thomas Telford, 1997.

[5.] Timoshenko, S. P. and Gere, J. M., *Theory of Elastic Stability 2/e*, McGraw-Hill., 1961

[6.] Brush, Don O. and Almroth, Bo O., *Buckling Analysis of Shells and Plate*, McGraw-Hill, 1975.

[7.] Grafton, P.E. and Strome D.R., Analysis of axisymmetric shells by direct stiffness method, *AIAA J.* 1, 2342-2347, 1963.

[8.] Zeinkiewicz, O.C., Bauer, J., Morgan, K. and Onate, E., A simple and efficient element for axisymmetric shells, *Int. J Num Meth. Eng.*, 11, 1545-1558, 1977.

[9.] Day, R.A. and Potts, D.M., Curved Midlin beam and axisymmetric shell elements- a new approach, *Int. J Num Meth. Eng.*, 30, 1263-1274, 1990

[10.] Park, K.H., A beam formulation for axisymmetric elasticity with arbitrary body force using particular integrals, *Computers and Structures,* 80, 2507-2514, 2002.

[11.] Gould, P.L. and Hara, T., Recent advances in local–global FE analysis of shells of revolution, *Thin Walled Structures*, 40, 641-649, 2002.

[12.] Liu, T., Kitipornchai, S. and Wang, C.M., Bending of linearly tapered annular mindlin plates, *Mechanical Science*, 43, 265-278, 2001.

[13.] Correia, I.F.P, Barbosa, J.I., Mota Soares, C.M. and Mota Soares, C.A., A finite element semi-analytical model for laminated axisymmetric shells: statics, dynamics and buckling, *Computers and Structures*, 76, 299-317, 2000.

[14.] Ding, K. and Tang, L., Exact solution for axisymmetric thick laminated shells, *Composite Structures*, 46, 125-129, 1999.

[15.] Benjeddou, A., Vibration of complex shells of revolutions using b-spline finite elements, *Computers and Structures*, 74, 429-440, 2000.

[16.] Haterbouch, M. and Benamar, R., Geometrically nonlinear free vibrations of simply supported isotropic thin circular plates, *J. Sound and Vibration,* 280, 903-924, 2005.

[17.] Elishakoff, I. and Storch, J.A., An unusual exact, closed-form solutions for axisymmetric vibration of inhomogenous simply supported circular plates, *J. Sound and Vibration.*

[18.] Zhou, D., Au, F.T.K., Cheung, Y.K. and Lo, S.H., Three-dimensional vibration analysis of circular and annular plates via the Chebyshev-Ritz method, *International Journal of Solids and Structures*, 40, 3089-3105, 2003.

[19.] Nasir, A.M., Thambiratnam, D.P., Butler, D. and Austin P., Dynamics of axisymmetric hyperbolic shell structures, *Thin Walled Structures,* 40, 665-690, 2002.

[20.] Cela, J.J.L., Huerta, C. and Alarcon, E., Numerical analysis of axisymmetric shells by one-dimensional continuum elements suitable for high frequency excitations, *Computers and Structures,* 78, 711-724, 2000.

[21.] Ley, R.P., Johnson, E.R. and Gürdal, Z., Buckling of imperfect, anisotropic, ring-stiffened cylinders under combined loads, *AIAA Journal*, 32, 1302-1309, 1994

[22.] Ma, L.S. and Wang, T.J., Relationships between axisymmetric bending and buckling solutions of FGM circular plates based on third-order plate theory and classical plate theory, *Int. J. Solids Structures,* 41, 85-101, 2004.

[23.] Wang; C. M., Member, ASCE, Xiang, Y., S. Kitipornchai, Fellow, ASCE, and Liew, K. M., Axisymmetric buckling of circular mindlin plates with ring supports, *Journal of Structural Engineering*, 119, 782-793, 1993.

[24.] Mermertaş, V. and Belek, H. T., Static and dynamic stability of variable thickness annular plates, *Journal of Sound and Vibration*, 141, 435-448, 1990.

[25.] Teng, J. and Rotter J. M., Buckling of pressurized axisymmetrically imperfect cylinders under axial loads, *Journal of Engineering Mechanics*, 118, 229-247, 1992.

[26.] Rao, P. S. and Ramanjaneyulu, K., Stability of cooling tower shell with modified wind pressure coefficients, *Journal of Engineering Mechanics*, 119, 2207-2225, 1993.

[27.] Sato, K., Elastic buckling of incomplete composite plates, *Journal of Engineering Mechanics,* 118, 1-4, 1992.

[28.] Singh, J. P. and Dey, S. S., Variational finite difference approach to buckling of plates of variable stiffness, *Computers and Structures*, 36, 39-45, 1990.

[29.] Zienkiewicz, O. C. and Campbell, J. S., Shape optimization and sequential linear programming, *Optimum Structural Design*. Eds. R. H. Gallagher and O. C. Zienkiewicz, Chapter 7, John Wiley, Chichester, 1973.

[30.] Mateus, H. C., Soares, C. M. and Soares, C. A., Buckling sensitivity analysis and optimal design of thin laminated structures, *Computers and Structures*, 64, 461-472, 1997.

[31.] Levy, R. and Spillers, W. R., Optimal design for axisymmetric cylindirical shell buckling, *Journal of Engineering Mechanics*, 115, 1683-1690, 1989.

[32.] Levy, R. and Ganz, A., Analysis of optimized plates for buckling, *Computers and_Structures*, 41, 1379-1385, 1991.

[33.] Pandey, M. D. and Sherbourne, A. N., Mechanics of shape optimization in plate buckling, *Journal of Engineering Mechanics*, 118, 1249-1266, 1992.

[34.] Lin, C. and Liu, I., Optimal Design for plate structures with buckling constraints, *AIAA Journal*, 28, 951-953, 1990.

[35.] Plaut, R. H., Johnson, L.W. and Parbery, R., Optimum forms of shallow shells with circular boundary Part 1-3, *Journal of Applied Mechanics*, 51, 526-539, 1984.

[36.] Olhoff, N. Optimal design of vibrating circular plates, *Int. J. Solids Structures*, 6, 139-156,1970.

[37.] Hamada, M., On the optimum shape of some axisymmetric shells, *Optimization in Structural Design*, Sawczuk, A. and Mroz, Z. (eds.), 248-262, Springer-Vrelag, Newyork, 1975.

[38.] Boisserie, J.M. and Glowinski, R., Optimization of thickness law for thin axisymmetric shells, *Computers and Structures*, 8, 331-343, 1978.

[39.] Mota Soares, C.M., Barbosa, J.I., Mota Soares, C.A and Pinto, P., Optimal design of axisymmetric shell structures, *FEMCAD*, 67-68, 1987.

[40.] Marcelin, J.L. and Trompette, P., Optimal shape design of thin axisymmetric shells, Engineering Optimization, 13, 109-117, 1988.

[41.] Mateus, H. C., Soares, C. M. and Soares, C. A., Buckling sensitivity analysis and optimal design of thin laminated structures, *Computers and Structures*, 64, 461-472, 1997.

[42.] Levy, R. and Spillers, W. R., Optimal design for axisymmetric cylindirical shell buckling, *Journal of Engineering Mechanics*, 115, 1683-1690, 1989.

[43.] Levy, R. and Ganz, A., Analysis of optimized plates for buckling, *Computers and Structures*, 41, 1379-1385, 1991.

[44.] Lin, C. and Liu, I., Optimal Design for plate structures with buckling constraints, *AIAA Journal*, 28, 951-953, 1990.

[45.] Richmond, A. and Azarkhin, A., Minimum weight axisymmetric structures, *Int. J. Solids Structures,* 42, 2439-2453, 2000.

[46.] Grafton, P.E. and Strome, D.R., Analysis of axisymmetric shells by the direct stiffness method, *AIAA Journal*, 1, 2342-2347, 1963.

[47.] Zienkiewicz, O.C. and Taylor, R.L., *The Finite Element Method*, Volumes I and II, Fourth edition, Mc-Graw Hill, New York, 1991.

[48.] Grould, P.L., *Finite Element Analysis of Shells of Revolution*, Pitman Publishing co., New York, 1985.

[49.] Hinton, E. Rao, N.V.R., Özakça, M., and Sienz, J., Optimum shapes for axisymmetric shells, *Proceedings of 4th International Conference on Non-linear_Engineering Computations*, Eds N. Bicanic, P. Marovic, DRJ. Owen, V. Jovic and A. Mihanovic, Swansea, U.K, 1991.

[50.] Hinton, E., Özakça, M., Optimum shapes of vibrating axisymmetric plates and shells", *Journal of Sound and Vibration*, 167, 511-528, 1993.

[51.] Özakça, M., Hinton, E., and Rao, N.V.R., Shape optimization of axisymmetric structures with adaptive finite element procedures, *Structural Optimization*, 5, 256-264, 1993.

[52.] Boresi A. P., Schmidt R. J., and Sidebottom O. M., *Advanced Mechanics of Materials 5/e*, Wiley, 1993.

[53.] Bathe, K. J._*Finite Element Procedures in Engineering Analysis*, Prentice-Hall, Englewood Cliffs, New Jersey, 1982.

[54.] Timoshenko, S.P. and Woinowsky-Kreiger, S., *Theory of Plates and Shells*, 2nd edition, McGraw-Hill, New York, 1959.

[55.] Tavakoli, M.S. and Singh, R., Modal analysis of a hermetic can, *J. Sound and Vibration*, 136, 141-145, 1990.

[56.] Carter, R.L., Robinson, A.R. and Schnobrich, W.C., Free vibrations of hyperboloidal shells of revolutions, *J. Engineering Mechanics*, 93, 1033-1053, 1969.

[57.] Tavakoli, M.S. and Singh, R., Eingen solutions of joined/hermetic shell structures using the state space method, *J. Sound and Vibration*, 100, 97-123, 1989.

[58.] Imam, M.H., Shape optimization of umbrella-shaped concrete shells subjected to self-weight as the dominant load, *Computers and Structures*, 69, 513-524, 1998.

[59.] Barbosa, J.I., Mota Soares,C.M., Mota Soares, C.A., Sensitivity analysis and optimal design of axisymmetric shells, *Computing Systems in Engineering*, 2, 525-534, 1991.

[60.] Thambiratnam, D.P. and Thevendran, V., Optimum vibrating shapes of beams and circular plates, *J. Sound and Vibration*, 121, 13-23, 1988.